Russian Chemical Reviews **65** (10) 825–847 (1996)
© 1996 Russian Academy of Sciences and Turpion Ltd

UDC 539.183:546

Inner valence molecular orbitals and the structure of X-ray photoelectron spectra

Yu A Teterin, S G Gagarin

Contents

I.	Introduction	825
II.	General notions	826
III.	Theoretical consideration	827
IV.	The structure of X-ray photoelectron spectra	830
V.	Contribution of inner valence molecular orbitals to chemical bonding	839
VI.	Conclusion	845

Abstract. X-Ray photoelectron spectroscopy (XPS) and theoretical calculations show that under certain conditions inner valence molecular orbitals (IVMOs) can form within a rather broad binding energy range (15 eV to 50 eV) in compounds of many elements of the Periodic Table. This results in the appearance of a fine structure in their X-ray photoelectron spectra. The structure of X-ray photoelectron spectra associated with electrons of IVMOs correlates with contributions of the filled atomic orbitals (AOs) to the IVMO formation and the structure of compounds. In certain cases, the total contribution of electrons of the inner valence molecular orbitals to the bond energy in molecules and compounds is comparable to that of electrons of the outer valence molecular orbitals. This phenomenon is extremely important and new in principle for chemistry. The bibliography includes 128 references.

I. Introduction

X-Ray photoelectron spectra of compounds of various elements of the Periodic Table often exhibit, instead of the expected atomic singlets and doublets associated with spin-orbital interaction, a more complicated structure. This spectral fine structure can appear due to the formation of molecular orbitals (MOs),[1–8] multiplet splitting, dynamic effect, multielectron excitation, etc.[7–10] Recently, much attention has been paid to the analysis of the reasons for the appearance of fine structure in X-ray photoelectron spectra of various compounds since it gives information on the physical and chemical properties and the structure of compounds, the nature of chemical bonds in them, oxidation states of constituent atoms, etc.[10–20] Although this problem is far from being completely solved, it becomes possible in certain cases to obtain unique information on compounds using the characteristics of the fine structure of X-ray photoelectron spectra.

Yu A Teterin Russian Research Centre 'Kurchatov Institute', Kurchatov sq., 1, 123182 Moscow, Russian Federation, Fax (7-095) 882 58 04.
S G Gagarin Fossil Fuel Institute, Ministry of Fuel and Energetics of the Russian Federation, Leninskii prosp., 29, 117910 Moscow, Russian Federation, Fax (7-095) 952 55 21

Received 18 December 1995
Uspekhi Khimii **65** (10) 895–919 (1996); translated by E F Valeev

Basically, the electrons of non-filled low-energy shells of neighbouring atoms (with energies ranging from 0 eV to ~15 eV) have been traditionally taken into account in spectral studies of the nature of chemical bonds. To some extent, it was facilitated by the widespread use of excitation sources of visible and UV-radiation in atomic and molecular spectroscopy. In most cases, X-ray emission spectroscopy studies of a wide range of compounds utilised the same interval of energies. Although, from the standpoint of quantum chemistry, the contribution of deep-lying filled atomic shells to the formation of MOs is well established,[21,22] it has been believed that the effect of these electrons on chemical bonding could be neglected compared to that of weakly-bound (from 0 eV to ~15 eV) electrons.

Progress in precision XPS, with soft X-ray radiation ($h\nu < 1.5$ keV) as a source of excitation, allowed the study of fine structure in the spectra of both weakly-bound and inner electrons. In X-ray photoelectron spectra of compounds taken in the interval from ~15 eV to ~50 eV, instead of separate lines associated with electrons of filled atomic subshells, a more complex structure attributed to electrons of MOs is observed.

Studies of the fine structure in X-ray photoelectron spectra of compounds of various elements of the Periodic Table have shown that, in many cases, rather strong interaction between the electrons of low-energy AOs, closed in the ground state, results in the formation of MOs lying in the energy range from 0 eV to ~50 eV.[1–8,11–16,23–28] This fact agrees with predictions of theoretical calculations.[29–33] Thus, clear experimental evidence of arrangement of filled AOs into MOs has been attained. However, the significant binding energy difference between certain pairs (bonding and antibonding) of low-lying MOs (from ~15 eV to ~50 eV) in some compounds allowed one to suggest that the perturbation induced by electrons of these MOs substantially affect bond strengths in these compounds.[1–6]

To this end, from the practical viewpoint, it is expedient to divide the X-ray photoelectron spectra into three regions depending on the electron binding energy. The first region (from 0 eV to ~15 eV) typically involves a poorly-resolved structure corresponding to the outer valence molecular orbitals (OVMOs), which are mainly built up of partially filled valence atomic orbitals. The second region (~15 eV ... 50 eV) exhibits a well-resolved structure associated with electrons of the inner valence molecular orbitals (IVMOs) which are mainly composed of closed atomic shells. Peaks that belong to the third region (more than 50 eV) reflect inner(core) MOs (CMOs) primarily consisting of deep-lying inner (core) AOs. However, due to the limited resolution of X-ray photoelectron spectrometers, separate peaks of electrons of

these CMOs cannot be observed even in the spectra of homonuclear gaseous molecules.[1] When we proceed to correlation of the structure of a compound with the structure of its IVMOs, the expedience of this division is most evident.

It should be noted that one cannot strictly divide MOs into categories of CMOs, IVMOs, and OVMOs, when considering the IVMO problem in general terms of the formation of MOs in various compounds. The character of the IVMOs in light-element compounds discussed in this review is closer to that of conventional OVMOs. Some of IVMOs of compounds containing heavy atoms are like CMOs. In other words, we should carefully consider this question for each particular compound. Moreover, although *de facto* the term 'IVMO' for light-element compounds has been used earlier, scientists started using this term for heavy-atom compounds only recently, since the existence of fine structure that could be interpreted in terms of the formation of IVMOs had been discovered in X-ray photoelectron spectra in the energy range of ~ 15 eV... ~ 50 eV.[2-6]

As has been mentioned in previous studies,[17,20] one of the reasons that a group of MOs referred to as IVMOs should be considered separately from the rest of MOs is that the peaks corresponding to IVMOs are well resolved, unlike those corresponding to OVMOs, and the fine structure associated with them depends on the nearest enviroment of the absorbing atom in the molecule or cluster. We should mention that, simultaneously with the appearance of a fine structure, multielectron effects can manifest themselves in the low-energy region of X-ray photoelectron spectra. It has been shown [1,17-20] that multielectron effects give rise to additional bands, as a rule, of much lower intensity than that of the major peaks, and a certain smearing of the spectrum. However, the spectral structure determined by the ground and final electronic states of the system with a vacancy after photoemission almost always remains firmly pronounced.

Fine structure observed in X-ray photoelectron spectra of shells of various compounds are evidence that multielectron effects play a noticeable role in their formation. However, one should keep in mind that XPS is of greatest practical use for a wide range of researchers when the spectra can be interpreted in terms of the one-electron approximation.

In the present review we discuss the IVMO problem from the general viewpoint. An attempt has been made to answer the following questions:

1. How common is IVMO formation for compounds of various elements of the Periodic Table?

2. What qualitative and quantitative information on physicochemical properties can be obtained from the spectral parameters of the IVMO-assigned fine structure?

3. How significant is the role of IVMOs in chemical bonding and what is the overall contribution of electrons of these orbitals to the covalent component of the bond energy?

For the sake of simplicity, we interpret the spectra containing fine structure using atomic notation as well as molecular ones.

II. General notions

In terms of the MO LCAO model, chemical bonding in diatomic molecules occurs by filling MOs with the common electrons. The positive, negative, or zero contribution of an electron to the bond energy depends upon the character of the corresponding MO (bonding, antibonding, or non-bonding). This concept was developed to the largest extent in the consideration of the nature of the chemical bond in diatomics, viz., homonuclear molecules of $D_{\infty h}$ symmetry and heteronuclear ones of $C_{\infty v}$ symmetry. The main qualitative postulate, which defines the relative bond energy in a diatomic molecule, is that the bond energy contributions of the electrons to the bonding and the corresponding antibonding MOs are approximately equal. The bond order, determining the bond strength, equals half the difference in populations of the bonding and antibonding MOs.[21,22,34-37] Therefore, the number of excessive 'bonding' electrons is considered to be the measure of the bond strength.[35,38-41] However, this rule is approximate,[21,35] since a molecule is destabilised by the electrons of antibonding MOs to a somewhat greater extent than stabilised by electrons of the corresponding bonding MOs.

The bonding or antibonding character of individual MOs can be established experimentally from the deviation, ΔR_e, of the internuclear distance from its equilibrium value in the ground state,[41,42] variations in dissociation energy ΔD_e,[37,41,43] and vibrational frequencies occuring due to the ionisation.[44] The MO character can be estimated roughly by consideration of the specific distribution of electron density in internuclear space [21] and on the basis of difference electron density maps $\Delta\rho$,[39] i.e. a difference between the molecular electron density and initial atomic electron densities.

As mentioned earlier,[21,22,34-41] the contributions of the electrons of the bonding and antibonding IVMOs to the covalent component of the bond energy compensate each other. Thus, the overall chemical bonding in a molecule is solely attributed to the electrons of OVMOs. Thus, it is believed that in a diatomic molecule AB of $C_{\infty v}$ symmetry, where A and B are second Period elements, as a first approximation, the bonding (3σ) and antibonding (4σ) IVMOs, which are composed of the $2s$ AOs of neighbouring atoms, in the first approximation do not affect the A–B bonding. Populations of the 1π, 5σ, and $2\pi^*$ OVMOs formed by the $2p$ AOs determine the total bond order. In homonuclear molecules A_2, such orbitals are classified as $2\sigma_g$ and $2\sigma_u^*$ IVMOs. The corresponding OVMOs within the framework of the D_{2h} symmetry point group are classified as the $1\pi_u$, $3\sigma_g$, and $1\pi_g$ outer valence molecular orbitals. This concept of the negligibly small influence of the electrons of MOs formed by doubly-occupied AOs on chemical bonding had been so widely used that it almost became an axiom. It is represented in a number of monographs [21,34,38,39,43,44] and textbooks for college students [35,37,40,41] and school teachers.[45,46] Until recently, attempts to revise this established model have hardly been undertaken.

However, the first *ab initio* calculations on the CO molecule (e.g., see review [47]) indicate either a weakly-bonding or antibonding character of the 5σ OVMO. The latter is usually used to explain the increased vibrational frequency of the CO^+ as well as $CO^{\delta+}$ ions, where $\delta+$ is a small charge induced upon the adsorption of the CO molecule on electron-deficient centres of a solid surface, compared to that of the neutral molecule. In an attempt to tailor this fact to a simple scheme of MO formation, the authors [44] assigned the bond order of the carbon-oxygen bond as 2 instead of 3, that is determined by four electrons in the 1π OVMO. It was considered that the electrons of the 3σ and 4σ IVMOs do not contribute to the chemical bonding owing to the mutual compensation of bonding and antibonding effects.

Another approach (see Refs 41, 44) implies a non-bonding character of the 3σ IVMO of the CO molecule (it is occupied by a lone electron pair of the O atom). The triple bond in the molecule is attributed to two electrons of the 4σ IVMO and four electrons of the 1π OVMO. In contrast, the authors of another study [21] assumed that the 4σ IVMO and 5σ OVMO are non-bonding, while the electrons in the 3σ IVMO and 1π OVMO account for the bond order 3.

Traditionally, triple bond formation in the CO molecule is attributed to the electrons of the $5\sigma^2$ and $1\pi^4$ OVMOs.[34,43] We should note that, according to the valence bond approach,[48] the bond order in the CO molecule is intermediate between 2 and 3 due to the contribution of resonance structures, namely, :C=:O: and :C≡:O.

Recently, attempts to quantify the bonding character of MOs in the CO molecule have been undertaken based on division of the total Hartree–Fock energy [49] and the values of Mulliken MO populations.[50] In these studies, the 3σ electrons were found to contribute significantly to the binding of C and O atoms in the CO molecule. Qualitative arguments in favour of the participation of the inner valence electrons in chemical bonding can be obtained by linear transformation of the 4σ IVMO and 5σ OVMO.[42] It has

been found that electrons occupying these MOs are essentially the lone pairs, and the $3\sigma(2\sigma_g)$ IVMO and $1\pi(1\pi_u)$ OVMO are involved in the triple bond formation in CO (or N_2).

Studies of the electronic structure of compounds by XPS [1-9,17-20,26-28] and theoretical calculations conducted at different levels of theory [3,4,29-32,49-57] have demonstrated that the conventional concept of the dominant participation of electrons of the OVMOs in chemical bonding is too rough an approximation.

III. Theoretical consideration

At present, there is no unified qualitative measure that allows the contribution of electrons of individual MOs to the bond strength, even for diatomic molecules, to be estimated. This quantity must be additive,i.e. the total bond energy must be equal to the sum of the individual MO contributions with respect to their populations. This condition is satisfied in the Mulliken bond population theory and in various quantum-chemical bond strength characteristics based on division of the total molecular energy into orbital and other components. Criteria concerned with an internuclear force, which arise due to changes in MO populations, are also of interest. This section discusses possible approaches to the solution of this problem.

1. Contribution of electrons to bond populations

In this approach, the contributions of electrons to the bond strength are estimated from Mulliken populations of MOs and AOs.[47] Within the MO LCAO approximation for a heteronuclear molecule AB, every pair of interacting orbitals satisfies the following equation:

$$\psi^{\pm} = \frac{1}{(2 \pm 2S)^{1/2}}(\chi^A \pm \chi^B), \tag{1}$$

where ψ^+ and ψ^- are the bonding and antibonding MOs respectively, χ^A (χ^B) an atomic orbital or, more generally, a linear combination of atomic orbitals of the atom A (B), and S is an absolute value of the overlap integral between χ^A and χ^B. The one-electron density in these MOs is defined as follows:

$$|\psi^{\pm}|^2 = \frac{1}{2(1 \pm S)}[|\chi^A|^2 + |\chi^B|^2] \pm \frac{1}{1 \pm S}\chi^A\chi^B. \tag{2}$$

The bonding space is an area between two planes passing through nuclei A and B perpendicularly to the bond axis. If χ is a non-hybrid AO, then the electron densities $|\chi^A|^2$ and $|\chi^B|^2$ contribute equally to the total electron density, not only in the bonding space, but also in the rest of space. The second term in Eqn (2) is the charge density localised essentially in the internuclear area. Therefore, one may consider this term as a qualitative measure of the bonding (antibonding) character of the MO. If ψ is the *sp* hybrid AO, then the first term in Eqn (2) also contributes to the bond order. The second term integrates to the following expression:

$$n(j_{\pm}, AB) = \pm\int \frac{1}{1 \pm S}\chi^A\chi^B d\tau = \pm\frac{S}{1 \pm S}, \tag{3}$$

which is the contribution of an electron in the *j*th MO to Mulliken's bond population. It follows from Eqn (3) that the contribution of an electron in the bonding MO ψ_i^+ is positive while the contribution of an electron in the antibonding MO ψ_i^- is negative and is larger in magnitude.

For diatomic heteronuclear molecules, the *j*th MO is expressed as:

$$\psi_j = c_j^A\chi^A + c_j^B\chi^B, \tag{4}$$

and the contribution of the electron in this MO to the bond population is:

$$n(j, AB) = 2c_j^A c_j^B \int \chi^A\chi^B d\tau. \tag{5}$$

Since the contributions are additive, the total population of the A–B bond is:

$$n(AB) = \sum_j N_j n(j, AB), \tag{6}$$

where N_j is the population of the *j*th MO.

In multiatomic molecules, $n(j, AB)$ refers to pairs of adjacent atoms. The partial contribution of an electron on the *j*th MO is defined as follows:

$$n(j) = \sum n(j, AB), \tag{7}$$

where the sum is taken over all the bonds.

2. Estimation of orbital character by separation of the total energy

Different kinds of interactions within the quantum-chemical approach are widely treated by separation of the total energy of a multiatomic molecule into one-, two-, three-, and four-centre components. The method of the complete neglect of differential overlap (CNDO/2)[55] serves as an example. The total energy E_{tot} within this method assumes the form:

$$E_{tot} = \sum_A E_A + \sum_{B,A} E_{AB}, \tag{8}$$

where E_A and E_{AB} are corresponding one- and two-centre components. The latter has the form:

$$E_{AB} = 2\sum_{\mu}^{A}\sum_{\nu}^{B} p_{\mu\nu}H_{\mu\nu} - \frac{1}{2}\sum_{\mu}^{A}\sum_{\nu}^{B} p_{\mu\nu}^2\gamma_{AB} + Z_A Z_B R_{AB}^{-1} - p_{AA}Z_B\gamma_{AB} - p_{BB}Z_A\gamma_{AB} + p_{AA}p_{BB}\gamma_{AB}, \tag{9}$$

where $p_{\mu\nu}$ is referred to as the bond order, the result of interaction of the μ-AO of atom A with the ν-AO of atom B; $H_{\mu\nu}$ are elements of the core Hamiltonian, γ_{AB} are repulsion integrals of the electrons of the *s*-type functions, Z_A (Z_B) is the charge of the nucleus (the effective value is used for the valence shell), p_{AA} (p_{BB}) is the electron density of the atoms.

The first term in Eqn (9) is referred to as the resonance energy.[56] Its magnitude characterises the covalent component of the A–B bond. The other terms denote the exchange component of the energy, core–core repulsion energy, potential energy of electrons of the atom A in the field of the core B, potential energy of electrons of the atom B in the field of the core A, and energy of electron–electron repulsion for atoms A and B respectively.

Despite the variational nature of the CNDO/2 approach, its semiempirical character does not yield total energy values that correspond to the results obtained with more rigorous approaches or from experiment. However, atomisation energies and bond energies of molecules can be estimated from components of the total energy in Eqn. (8).[57] It will be shown (see Section V.1) that the results of CNDO/2 calculations can provide an estimate of the bonding character of MOs. To this end, the resonance energy E_{AB}^R is separated into contributions E_α^R of individual MOs:

$$E_{AB}^R = \sum_\alpha E_\alpha^R,$$

$$E_\alpha^R = 2n_\alpha \sum_i^A \sum_j^B c_{i\alpha}c_{j\alpha}H_{ij}, \tag{10}$$

where n_α is the population of the α MO, H_{ij} the core Hamiltonian, $c_{i\alpha}$ and $c_{j\alpha}$ are the coefficients of the ith and jth AOs in an expansion of the α MO by atomic orbitals found from self-consistent field (SCF) calculation, CNDO/2. The positive (negative) sign of the contribution E_α^R to the resonance energy corresponds to the antibonding (bonding) character of the α MO.

3. Estimation of the orbital character within the orbital force approach

According to the Hellmann–Feynman theorem, the internuclear force is equal to the expectation value of $\partial\hat{H}/\partial R$, where $\hat{H}$ is the Hamiltonian and R is the internuclear distance.

Forces acting on nuclei in a molecule are determined as derivatives of the potential energy with respect to internal bond lengths and bond angles or cartesian coordinates. These forces can also be calculated from the known wave functions. Regarding a diatomic molecule AB, the total force acting on the nucleus A is:

$$F_A(R) = \frac{Z_A}{R^2}\left(Z_B - n_e R^2 \int \psi_{AB}^* \frac{\cos\theta_{\mu A}}{r_{\mu A}^2}\psi_{AB}\mathrm{d}\tau\right), \tag{11}$$

where n_e is the total number of electrons, R is the internuclear distance, μ is the electron index, A is the atom index, $r_{\mu A}$ is the distance from the μth electron to the nucleus A, $\theta_{\mu A}$ is the angle between the bond direction and radius-vector of the μth electron of the atom A, $\mathrm{d}\tau$ is the space unit. At $R = R_e$, $F_A = -F_B = 0$, therefore the second term in Eqn (11) must be equal to Z_B, i.e.

$$n_e R_e^2 \int \psi_{AB}^* \frac{\cos\theta_{\mu A}}{r_{\mu A}^2}\psi_{AB}\mathrm{d}\tau = Z_B. \tag{12}$$

This term reflects the contribution of electrons to the total force acting on the nucleus. Within the MO LCAO approach, the following expression is valid for each MO:

$$\eta_i = R^2 N_i \int \phi_i^* \frac{\cos\theta_{\mu A}}{r_{\mu A}^2}\phi_i \mathrm{d}\tau, \tag{13}$$

where ϕ_i is the MO , N_i is the number of electrons in the ith MO. Subject to Eqns (12) and (13), it follows that:

$$\sum_i \eta_i = Z_B, \tag{14}$$

where the integration is performed over the occupied MOs.

A modified orbital force f_i, which determines a one-electron contribution to the total force,[17] can be introduced

$$f_i = \frac{Z_B}{N_i R^2}\eta_i, \tag{15}$$

This force is also additive, i.e.

$$\sum_i N_i f_i = \frac{Z_B^2}{R^2}. \tag{16}$$

The force f_i can be calculated from the derivative of the orbital energy vs. the internuclear distance. Indeed, according to the Fock equation for the MO

$$\hat{F}\phi_i = E_i\phi_i, \tag{17}$$

it follows that:

$$E_i' = \frac{\mathrm{d}E_i}{\mathrm{d}R} = \int \phi_i^* \left|\frac{\mathrm{d}\hat{F}}{\mathrm{d}R}\right| \phi_i \mathrm{d}\tau. \tag{18}$$

Since

$$\hat{F} = \hat{h} + G,$$

where $\hat{h}$ is the one-electron Hamiltonian, $\hat{G}$ is the operator of the electron–electron electrostatic interaction, then

$$E_i' = f_i + \int \phi_i^* \left|\frac{\mathrm{d}\hat{G}}{\mathrm{d}R}\right| \phi_i \mathrm{d}\tau. \tag{19}$$

According to Eqn (19), f_i differs from E_i' only by electron–electron repulsion terms. These terms can be estimated using the values of E_i' and f_i listed in Table 1.

Presumably, the second term in Eqn (19) equals f_i times a constant factor. Then Eqn (19) takes the form:

$$E_i' \simeq f_i + cf_i = (1 + c)f_i. \tag{20}$$

A correlation plot of E_i' versus f_i using the data in Table 1 proves this assumption (Fig. 1). According to this plot, the coefficient c equals approximately 0.23. Therefore, Eqn (20) may be rewritten:[17]

$$E_i' \simeq 1.23 f_i. \tag{21}$$

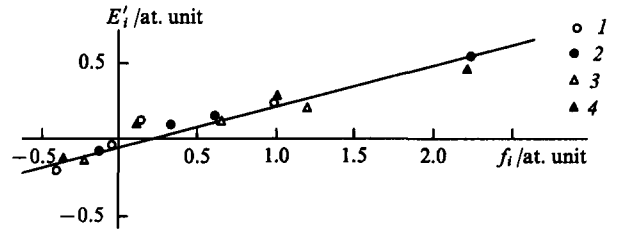


Figure 1. Dependence of the derivatives of the orbital energies E_i' on the orbital forces f_i for: (*1*) O_2; (*2*) B_2; (*3*) C_2; (*4*) N_2 (1 at. unit = 8.24×10^{-8} N).[17]

The orbital forces can be substituted by E_i' values in a semiquantitative estimation of the relative contributions of electrons of individual MOs to the covalent bonding, since the total covalent component of the bond energy of the molecule can be represented as the sum of the orbital energies with respect to their populations.[59] Ruedenberg[60] has suggested an empirical correlation between the total covalent component of the Hartree–Fock energy E of a molecule and the sum of the orbital energies of the occupied MOs:

$$E \simeq k\sum_i N_i E_i, \tag{22}$$

where k is a constant.

Table 1. The orbital forces f_i and derivatives of the MO energies (E_i' /10^{-8} N).[17]

Molecule	$2\sigma_g$ IVMO		$2\sigma_u$ IVMO		$1\pi_u$ OVMO		$3\pi_g$ OVMO		$1\pi_u$ OVMO	
	E_i'	f_i	E_i'	f_i	E_i'	f_i	E_i'	f_i	E_i'	f_i
B_2	0.824	5.257	−0.585	−1.121	0.634	2.711	–	–	–	–
C_2	1.524	10.086	−1.162	−1.953	1.038	5.043	–	–	–	–
N_2	3.486	18.087	−1.195	−3.123	2.175	8.199	0.709	1.014	–	–
O_2	4.227	18.573	−1.640	−3.280	1.838	8.240	1.129	1.104	−1.607	2.694

From Eqn (22),

$$F = -\frac{\partial E}{\partial R} \cong -k\sum_i N_i E_i'. \quad (23)$$

Roedenberg's value[60] 3/2 for k in Eqn (22) differs somewhat from 1.23 in Eqn (21). Apparently, the coefficient in Eqn (21) varies for series of diatomic molecules made up of elements of different Periods. The same is valid for the constant k in Eqn (22). Goscinsky[61] also noted the approximate character of the estimation of the orbital forces from E_i'. He suggested a technique for calculation of the derivatives, which takes into consideration the MO relaxation occuring during the ionisation of a molecule. According to this approach, a force arising on nuclei due to the removal of an electron from the ith MO equals the derivative of the energy of the ion (i) with respect to the internuclear distance at the equilibrium point of the initial molecule:

$$\tilde{f}_i = -\frac{dE_i^i(R)}{dR}\Big|_{R_e}. \quad (24)$$

Koopmans's theorem states that

$$E_i^i(R) = E(R) - E_i(R), \quad (25)$$

where $E(R)$ is the total energy of the ground state of the molecule. Then within this approach,

$$\tilde{f}_i = E_i'. \quad (26)$$

Taking into account MO reorganisation caused by a change in the populations, we obtain:

$$\tilde{f}_i = E_i' + \frac{dE_i^{rel}(R)}{dR}\Big|_{R_e}, \quad (27)$$

where $E_i^{rel}(R)$ is the relaxation energy of the system upon removal of an electron from the ith MO. A method for the determination of the contribution of MO relaxation within the transition operator approach has been suggested.[61]

The effect of relaxation is automatically taken into account if orbital forces are determined from experimental rather than the calculated spectral data.[62] In this case, the orbital forces are referred to as the orbital vibronic constants.[63,64,65] A deformation force, which arises on nuclei upon vertical electron excitation or ionisation of a diatomic molecule, is determined as a derivative of the potential energy of the final state versus the interatomic distance at the transition point. For a Morse potential we may write[21]

$$U(x) = D_e[\exp(-2\beta x) - 2\exp(-\beta x)], \quad (28)$$

where D_e is the depth of the well, β is a variable parameter, and x is the deviation of the interatomic distance R from its equilibrium value R_e. Then the classical force $\tilde{f}$ is determined as follows:

$$\tilde{f} = -\frac{dU(x)}{dx}\Big|_{x^*} = -2D_e\beta[\exp(-\beta x^*) - 2\exp(-2\beta x^*)], \quad (29)$$

where x^* is the difference between the equilibrium distances in the initial and final states.

4. Relationship between various characteristics of the orbital contributions

Most simply, the estimation of the MO contribution to the bonding is determined as a part of the Mulliken bond population associated with this MO. The values of the bond populations for a series of diatomic molecules and the values of the orbital forces for some of them[47] are listed in Table 1. Correlation plots of the bond population vs. the orbital force f_i for the valence MOs of C_2, N_2, and O_2 shown in Fig. 2 yield straight lines. This reflects the approximate character of the bond order as an index of the bond

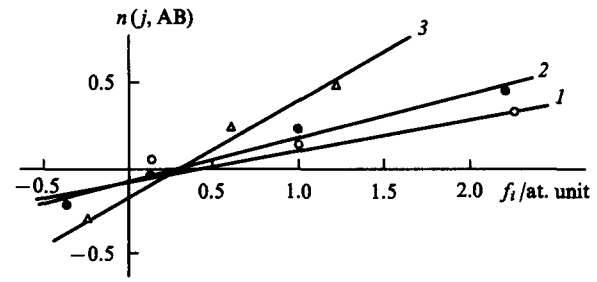


Figure 2. Dependence of the bond populations $n(j; AB)$ on the orbital forces f_i for valence MOs of (*1*) O_2, (*2*) N_2, and (*3*) C_2.[65]

strength. We have to note that only the MO contributions to the bond order $n(j, AB)$ calculated within the extended Hückel approach correlate satisfactorily with other characteristics, such as the orbital forces f_i, and the orbital vibronic constants for MOs of the same molecule.[17] The CNDO/2 calculations for N_2, CO, NO, O_2, C_2, and CN have been carried out in order to test whether the bonding character of MOs can be estimated from values of the orbital resonance energy.[65] For the first four molecules, the orbital vibronic constants, which had been calculated earlier from spectral data,[62] were used as the bonding indices. The values of the orbital vibronic constants for the last two molecules were calculated from the corresponding wave functions of OVMOs.[62] The total number of data points reached 20. The correlation between the CNDO/2 resonance orbital energies and the orbital vibronic constants has been established (Fig. 3). Characteristically, the plot yields a straight line through the origin of coordinates, and the correlation has the form:

$$a_\alpha = -7.1E_\alpha^R, \quad (30)$$

where a_α is the orbital vibronic constant (in 10^{-8} N) and E_α^R is the resonance orbital energy in atomic units. The orbital vibronic constants of arbitrary MOs can be calculated from the orbital contribution to the resonance energy using this dependence. In particular, it makes possible the determination of the orbital vibronic constants of IVMOs for which spectral data are currently unavailable.

Ab initio calculations of the electronic structure of molecules N_2,[66,67] CO,[67,68] and a radical CH[69] have provided the values of derivatives (E_α') at the equilibrium interatomic distances. Graphical analysis reveals a correlation between E_α' and a_α of the form:

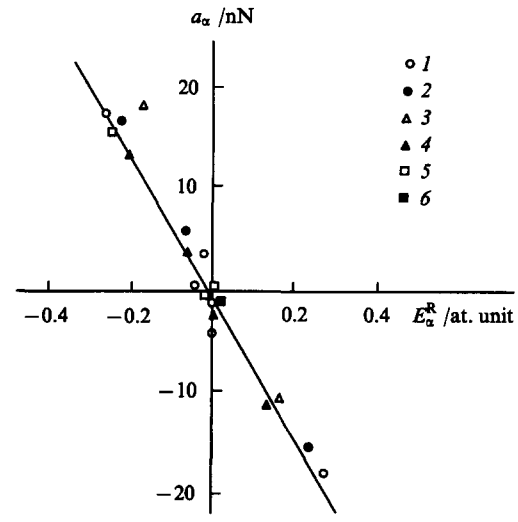


Figure 3. Dependence of the orbital vibronic constants a_α on the orbital resonance energies E_α^R for: (*1*) N_2; (*2*) CO; (*3*) O_2; (*4*) NO; (*5*) CN; (*6*) C_2.[65]

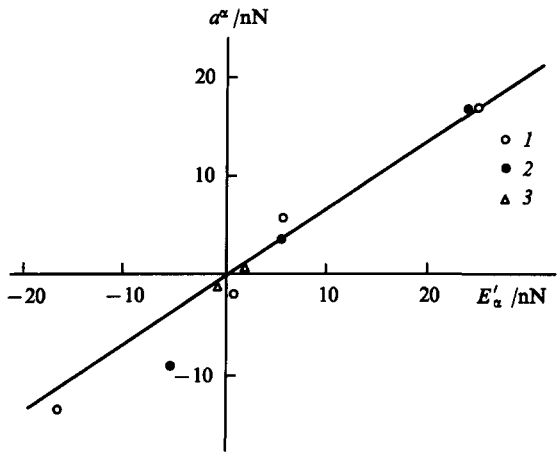


Figure 4. Correlation of the orbital vibronic constants a_α with the derivatives of the MO energies E'_α for: (*1*) CO; (*2*) N_2; (*3*) CH.[65]

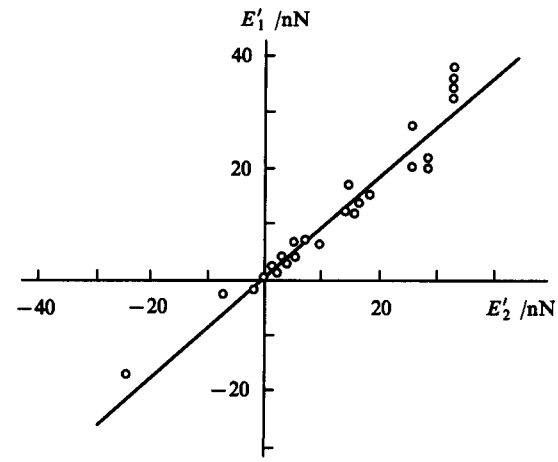


Figure 5. Correlation of the derivatives of the orbital energies E'_1 obtained from *ab initio* calculations with those, E'_2, obtained from SCF CNDO/2 calculations for N_2, CO, CH, LiH, BeH, BH, NH, and HF.[70]

$$a_\alpha = 0.71E'_\alpha, \tag{31}$$

where both E'_α and a_α are expressed in nN (Fig. 4). Obviously, Eqn (31) can also be applied to calculations of the missing orbital vibronic constants. We should keep in mind that formula (31) was derived with a limited number of data points due to incomplete sets of experimental a_α values rather than due to the absence of *ab initio* studies with varied R.[62] Consequently, an examination of the correlation between E'_α and E^R_α would be helpful for verification of Eqn (31). This challenge is feasible since non-empirical $E_\alpha(R)$ dependences have been published for a number of diatomic molecules and the corresponding CNDO/2 values of E^R_α can be readily calculated. With this in mind, we appended the values of the orbital energy derivatives from *ab initio* calculations for molecular hydrides LiH, BeH, BH, NH, and HF[69,70] to the list of those for N_2, CO_2, and CH, so that the total number of data points reached 32. From least-squares analysis of the data collected

$$E'_\alpha = b_0 + b_1 E^R_\alpha$$

the coefficients b_0 and b_1 were found to be equal to 0 and −10 respectively. Thus the correlation between the non-empirical derivatives of the orbital energies and the semiempirical values of the orbital resonance energies has the form:

$$E_\alpha{}' = -10E^R_\alpha. \tag{32}$$

Composition of Eqns (32) and (30) corroborates Eqn (31). Also, it can be demonstrated that the CNDO/2 derivatives of the orbital energies are of certain interest for the estimation of orbital vibronic constants. Indeed, reasoning by analogy with Eqn (32), we have

$$E'_\alpha(\text{CNDO/2}) = -10.9E^R_\alpha. \tag{33}$$

On other hand,

$$a_\alpha = 0.65E'_\alpha(\text{CNDO/2}). \tag{34}$$

The last two dependencies corroborate additionally the validity of Eqn (30). It can be deduced from Eqns (33) and (34) that the non-empirical and CNDO/2 values of E'_α correlate. The dependence presented in Fig. 5 confirms this expectation.

According to the data mentioned above, derivatives of the orbital energy versus the internuclear distance can serve as an estimate of orbital vibronic constants in diatomic molecules.[17] It is not surprising that CNDO/2 values are successfully used on even terms with non-empirical data since the initial parametrisation of the semiempirical method employed *ab initio* data for small molecules. At the same time, the derivatives E'_α obtained in terms of the extended Hückel method correlate with the orbital vibronic constant to a lesser extent although satisfactory results can still be obtained in certain cases. The same holds for the correlation between the orbital vibronic constants and the Mulliken orbital populations (Fig. 6).

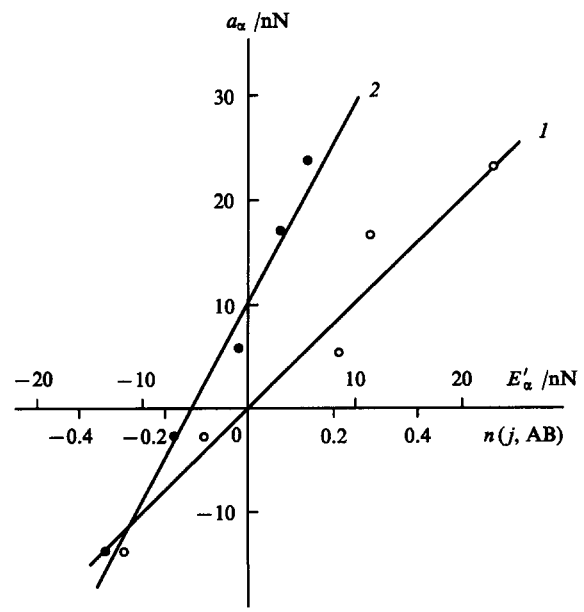


Figure 6. The orbital vibronic constants a_α for the CO molecule as functions of the bond strength indexes calculated within the extended Hückel approach: (*1*) $n(j;AB)$; (*2*) E'_α.[17]

IV. The structure of X-ray photoelectron spectra

X-Ray photoelectron spectroscopy is based on the photoeffect.[1] Under exposure to exciting X-ray radiation, e.g., $MgK_{\alpha 1,2}$, photoelectrons with kinetic energy of up to ~1.2 keV are emitted. The electron energy is measured to an accuracy of 0.1 eV. As a result, the binding energies (electronic work functions) of inner and outer levels of the coumpound under examination can be determined up to a constant factor from the Einstein equation.

An X-ray photoelectron spectrum represents the number of photoelectrons (peak intensity I expressed in relative units) plotted against the binding energy E_b (in eV). To enable compar-

ison of X-ray photoelectron spectra, they are calibrated against a known value of the binding energy E_b of electrons of a certain shell of a standard substance, e.g., gold (Au $4f_{7/2}$).

The X-ray photoelectron spectra of the compounds to be discussed in this review were obtained in the gas phase [1] and solid state.[17-20] High-resolution spectra of solid compounds are usually obtained with the monochromatic Al$K_{\alpha 1,2}$ (1486.6 eV) characteristic X-ray radiation and a low-energy electron gun. Samples are usually prepared as dense layers precipitated from inert solvents or depressed on an indium support. Experiments are carried out either at ambient or liquid-nitrogen temperatures. All the spectra discussed are reduced to the same scale in which the binding energy E_b of the C 1*s* electrons in hydrocarbons was set equal to 285.0 eV (except for gas-phase spectra).

Fine structures in X-ray photoelectron spectra are often interpreted using calculations of the electronic structure of molecules and clusters performed mainly by non-relativistic SCF methods, namely, the SCF CNDO/2, SCF Xα-SW,[29,55,71-75] and SCF Xα-DV.[31,32,76-80]

The formation of IVMOs between neighbouring atoms requires that:

(a) the energies of the corresponding filled AOs are comparable;

(b) these AOs possess the same symmetry type with respect to the interatomic axis;

(c) the interatomic distance is sufficient for effective overlap of these AOs.[17,21,81-85]

According to (a) and (b), it is anticipated that IVMOs effectively form in homonuclear molecules, and, with (c) satisfied, IVMOs can form in heteronuclear compounds too.

Such difficulties as fast oxidation and decomposition of highly-reactive compounds as well as the influence of aggressive species, e.g. F_2, Cl_2, etc., on units of the spectrometer often arise in XPS studies of these compounds, for which the formation of IVMO is expected. Generally, these difficulties are not fundamental since the current level of the experimental technique is sufficient to overcome such problems. However, XPS studies are preferably performed with stable inert compounds to obtain the most reliable results. It is the main factor that defines up to now the set of available spectra of homo- and heteronuclear compounds.

We should also mention that solid compounds form a lattice where electronic states are described in terms of the band structure. In a certain approximation, the bands represent MOs, thus they reflect the electronic structure of clusters typical of a given compound in the solid phase. This seems to be quite admissible for the less-delocalised core electrons, and the corresponding peaks in X-ray photoelectron spectra are broadened. Such broadening due to effects of the solid lattice gives maxima, attributable to the band structure, which are referred to as peaks for the sake of simplicity and attributed to electrons of individual clusters.

In this review we discussed X-ray photoelectron spectra of compounds of group IVA – VIIA elements, lanthanide oxides and fluorides (except for Pm compounds), and a wide range of actinide series compounds.

1. Manifestation of inner valence molecular orbitals in X-ray photoelectron spectra

a. Homonuclear molecules and clusters of group IVA – VIIA elements

X-Ray photoelectron spectra of solid compounds under consideration reveal a fine structure occurring in the low-energy region. Since the electronic configuration of these elements is ns^2np^m, where $2 \leqslant m \leqslant 5$, this fine structure can be concerned considerably with the interaction of *ns* electrons. A simpler fine structure appears in the spectra of gaseous diatomic molecules of these elements (Fig. 7). In this case, on the one hand, homonuclear molecules provide the most favourable conditions for IVMO formation; on the other hand, rigorous theoretical studies of the electronic structure of these compounds can be performed and interpreted relatively easily.

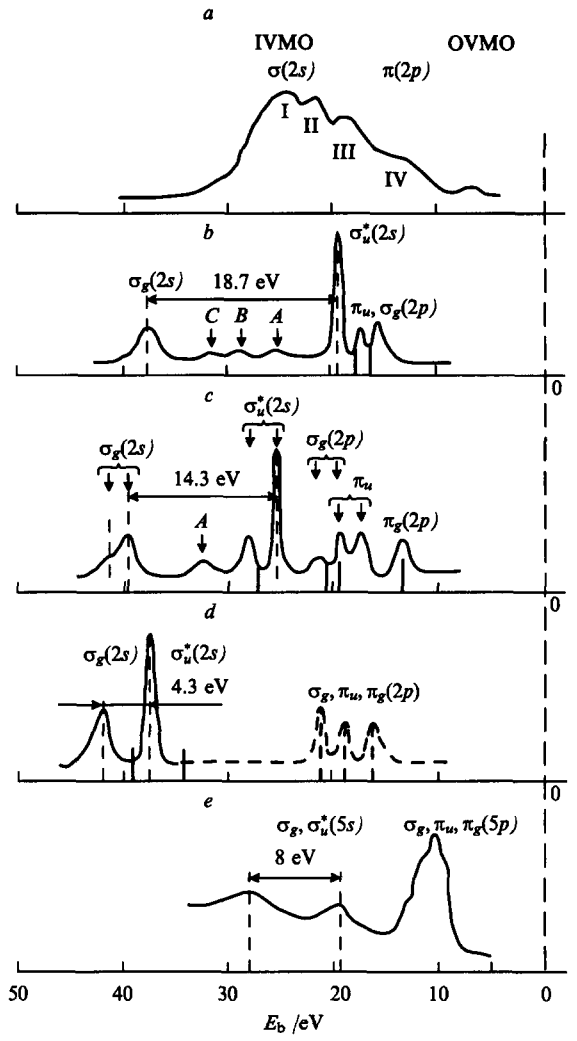


Figure 7. The X-ray photoelectron spectra of pyrographite (E_b(C1*s*) = 290 eV) (*a*)[25] and gaseous N_2 (*b*),[1] O_2 (*c*),[1] F_2 (*d*),[23] and I_2 (*e*).[24] The bond lengths (in Å) are 1.42 (C–C), 1.098 (N≡N), 1.207 (O=O), 1.417 (F–F) and 2.666 (I–I).

The results of the CNDO/2 and Xα-DV theoretical calculations [1,32,51,56,86,87] for the N_2 molecule, establish that the two most intense low-energy peaks in the X-ray photoelectron spectra of this molecule, separated by 18.7 eV, are associated essentially with the electrons of the antibonding $2\sigma_u^*$ and bonding $2\sigma_g$ IVMOs. The calculated gap (ΔE_{theor}) between the binding energies of electrons of the $2\sigma_g$ and $2\sigma_u^*$ IVMOs in the N_2 molecule equals 16.9 eV (Xα-DVM) and 18.1 eV (CNDO/2) at the equilibrium distance $R_e = 0.109$ nm.[51,56] The fine structure of the X-ray photoelectron spectrum of N_2 theoretically modelled at the SCF Xα-DVM level (bond length $R = 0.106$ nm, $\Delta E_{theor} = 18.59$ nm) is shown in vertical lines below the experimental spectrum (Fig. 7 *b*). The scales of the experimental and theoretical spectra do not match; the binding energy differences of the N 1*s* electrons are not equal ($|E_{exp}(N\,1s) - E_{theor}(N\,1s)| = 7.5$ eV). Additional peaks (*A*, *B*, and *C*) attributable to multielectron effects, characteristic losses, and Mg$K_{\alpha 3,4}$ excitation appear in the X-ray photoelectron spectrum of N_2.[1] The spectrum of the weakly-bound electrons of the nitrogen molecule is an examplary demonstration of IVMO formation in molecules.

The spectrum of the O_2 molecule provides yet another example.[1] In the low-energy region of its spectrum, as in the spectrum of N_2, two peaks associated with electrons of the $2\sigma_g$ and $2\sigma_u^*$ IVMOs appear; the binding energy gap ΔE_{exp} between them equals 14.3 eV (Fig. 7 *c*). These IVMOs to a great extent consist of the O 2*s* AOs. Since O_2 is paramagnetic, multiplet splitting of the electronic states appears in the spectrum. Thus, every peak except for one of the π_g^* electrons is split into two components corresponding to the $^2\Sigma^-(^2\Pi)$ and $^4\Sigma^-(^4\Pi)$ possible electronic states of the system after electron photoemission. Additional peaks (*A*, *B*,...) associated with multielectron effects, characteristic losses, and the Mg$K_{\alpha 3,4}$ excitation are present in the O_2 spectrum as well as in the spectrum of N_2.[1] The theoretically predicted spectrum obtained within the framework of the SCF Xα-DVM approach[32] is represented by vertical lines in Fig. 7 under the experimental one.

Theoretical predictions of X-ray photoelectron spectra of diatomic molecules, namely N_2, CO, O_2, NO, etc., taking into account multielectron effects demonstrate that configuration interaction somewhat complicates the spectra calculated within the one-electron approximation.[1] However, one-electron spectra can be used in considering the IVMO formation since they are much like the experimental spectra.

The binding energy difference between electrons of the $2\sigma_g$ and $2\sigma_u^*$ IVMOs in the F_2 molecule is essentially smaller than those in N_2 and O_2 and equals $\Delta E_{exp} = 4.28$ eV.[23] The results of the SCF Xα-DV calculation[32] of the electronic structure for the F_2 molecule ($\Delta E_{theor} = 5.6$ eV) are shown in Fig. 7 *d* and compared with the experimental spectrum. Another detailed study on the IVMO formation in the F_2 molecule, in which the contribution of the IVMO electrons to the bond energy was estimated, was accomplished at the SCF Xα-SW level of theory.[73]

There is a slight difference between the low-energy part of the spectrum of molecular iodine in gaseous and condensed states.[24] In the region of the I 5*s* electrons (~15 eV–35 eV), two broadened peaks are present in both spectra.[24] These peaks are attributed to the σ_g and σ_u^* IVMOs that refer to the I 5*s*–5*s* interaction. The energy difference between these IVMOs is of about 8 eV (see Fig. 7), although the bond in the I_2 molecule is relatively long ($R_e = 0.2666$ nm) to result in such a considerable difference in energy. Therefore, it was hypothesised[17] that the energies of these IVMOs differ much less and the peaks associated with them appear at around $E_b = 19$ eV. However, this assumption still has to be confirmed by theoretical calculations.

The calculated electronic structure of the C_2 molecule[88] implies also an essential feature of the C 2*s*–C 2*s* overlap resulting in the formation of the $2\sigma_g$ and $2\sigma_u^*$ IVMOs. At the interatomic distance $R_e = 0.1242$ nm, the binding energy difference between electrons of the $2\sigma_g$ and $2\sigma_u^*$ IVMOs is 18.2 eV, which substantially extends the energy range of the X-ray photoelectron spectrum of C_2 compared to the atomic spectrum of carbon. This accounts for a larger width (~25 eV)[17,25] of the low-energy band in highly-oriented pyrolitic graphite (Fig. 7 *a*) and diamond compared to the width of the valence band in solid Si and Ge, which possess the diamond-type structure.[17] Since the X-ray photoelectron spectra of graphite and diamond recorded in this region are essentially associated with the C 2*s* electrons,[17,25] it was postulated[88] that the base of the valence band is strongly lowered due to the IVMO formation by the C 2*s* AOs.

Peaks attributed to electrons of the IVMOs arising mainly from the *ns*–*ns* interaction are also present in X-ray photoelectron spectra of other homonuclear compounds of Group IVA–VIIA elements (see Refs 17, 52, 72 and Figs 8 and 9). The binding energy difference between the electrons of the IVMOs decreases as the atomic number *Z* increases.[17,20] In other words, the character of the IVMOs is getting closer to that of the inner (core) MOs, i.e. the overlap between occupied and vacant valence AOs decreases. A similar tendency in the formation of IVMOs is observed when the atomic number insreases in a Period.

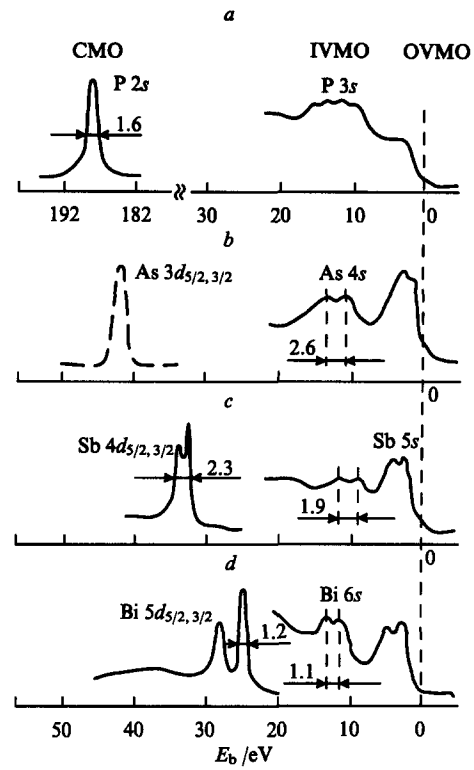


Figure 8. The X-ray photoelectron spectra of red phosphorus (*a*), As (*b*),[11] Sb (*c*), and Bi (*d*) in the solid state.[72] Here and elsewhere the CMO and IVMO spectra are not calibrated in terms of intensity. In this case, for phosphorus, the intensity of the CMO spectrum is 15 times that of the IVMO one; the intensity of the CMO spectra of As, Sb and Bi is 20 times that of the IVMO one.

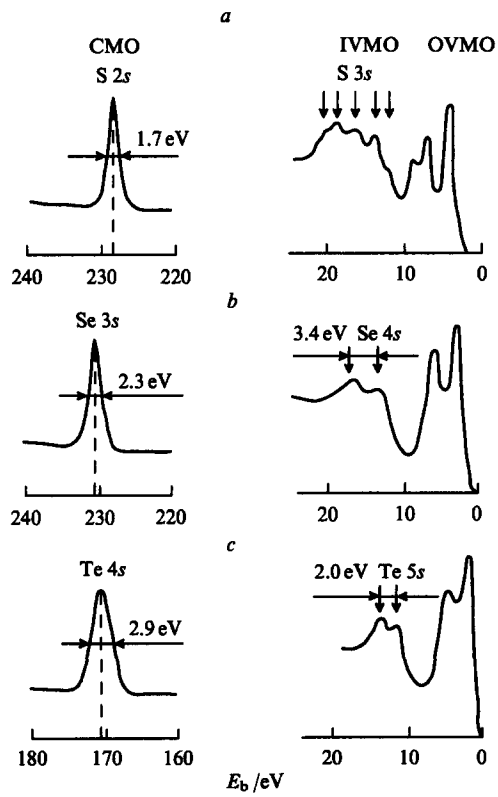


Figure 9. The X-ray photoelectron spectra of solid S (*a*), Se (*b*), and Te (*c*).[52]

b. Heteronuclear compounds of group IVA – VIIA elements

In some cases, the very fact of the formation of IVMOs in heteronuclear compounds as well as in homonuclear ones can be established definitely on the basis of characteristics of the fine structure in their X-ray photoelectron spectra. It becomes feasible since IVMO formation does not lead to an appearance of separate peaks, but to a complex fine structure in the energy range of ~15 eV to ~50 eV of the X-ray photoelectron spectra of a heteronuclear compound. Separate peaks can often be classified as being associated with the electrons of IVMOs based on the cooperative analysis of characteristics of the fine structure in spectra of inner and outer electrons. The X-ray photoelectron spectra can then be interpreted qualitatively in terms of group theory. However, in certain cases, especially if electrons of AOs contributing to the IVMOs have significantly different photoionisation cross-sections, a rigorous assignment of the peaks attributed to these MOs can be performed with the aid of theoretical calculation. Thus, the O 2*s* peak in the X-ray photoelectron spectrum of SiO_2 has a shoulder on its high-energy slope and it is significantly broadened (Fig. 10). This structure of the spectrum of O 2*s* cannot be attributed to the participation of the oxygen atoms in different types of chemical bonding since the spectrum of O 1*s* electrons consist of one, relatively narrow peak. The electronic structure of the $Si_2O_7^{6-}$ cluster calculated at the SCF Xα-DV level [17] points to a noticeable interaction between the electrons of the Si 3*s* and O 2*s* AOs resulting in IVMO formation (Fig. 10). This result agrees with published data.[33]

A complex structure is observed in the F 2*s* region of the X-ray photoelectron spectra of compounds $[CpMn(CO)_2NO]^+PF_6^-$, $[CpMn(CO)(NO)PPh_3]^+PF_6^-$, and $[CpMn(NO)(PPh_3)_2]^+PF_6^-$, where Cp is cyclopentadienyl (Fig. 10).[17] This structure cannot be attributed to the fluorine atoms with different effective charges since the F 1*s* electrons are represented with one symmetrical, relatively narrow peak. Thus, it was suggested [17] that the structure of the F 2*s* peak of the PF_6^- cluster can be partially assigned to the interaction between the F 2*s* and P 3*s* AOs resulting in IVMO formation.

An analogous peak profile is observed in the F 2*s* region of the X-ray photoelectron spectrum of SF_6. Its three components are identified as the $1a_{1g}$, $1t_{1u}$, and $1e_g$ MOs (in descending order of the absolute energy values).[1] These orbitals comprise the F 2*s* and S 3*s*, F 2*s* and S 3*p*, and F 2*s* and F 2*p* AOs to an extent of 64 and 33, 77 and 20, and 98 and 2 percent respectively. Since the electron configurations of sulfur $\{3s^23p^4\}$ and phosphorus $\{3s^23p^3\}$ atoms are similar, the X-ray photoelectron spectrum of the PF_6^- cluster has been interpreted by analogy with the SF_6 spectrum.

Instead of an expected single peak, two peaks of electrons of the $1a_1$ and $1t_2$ IVMOs are observed in the X-ray photoelectron spectrum of gaseous CF_4. These MOs consist of the F 2*s* and C 2*s* AOs to an extent of 69 and 27, and 82 and 15 percent respectively. A fine structure associated with electrons of the filled AOs, which take part in the IVMO formation, also appear in the X-ray photoelectron spectra of NO, CO, CH_3OH, H_2O, and H_2S.[1] It has been noted [74,89] that the structure of the O 2*s* region of the X-ray photoelectron spectra of the MO oxides, where M denotes Ca, Sr, and Ba, is associated with the IVMOs made up partially of the M *np* and O 2*s* AOs of neighbouring atoms. This is consistent with the results of an electronic structure calculation for the CaO_6^{10-} of O_h symmetry (the SCF Xα-SW method was used).[74]

The interpretation of fine structure in the low-energy region of the X-ray photoelectron spectra of La-, Y-, Bi-, and Tl-based high-temperature superconductors [90–92] has revealed that IVMOs form in these due to interaction between the O 2*s* AOs and the closest-in-energy-shell of metal atoms in these compounds. Previously,[93,94] the fine structure in the X-ray photoelectron spectra of these compounds led to the hypothesis that all the elements in high-temperature superconductors possess shells with energies close to that of the O 2*s* AO. Then, by correlation of the oxidation state of metal ions with their radii, the range of elements that can form HTSC has been defined.[93]

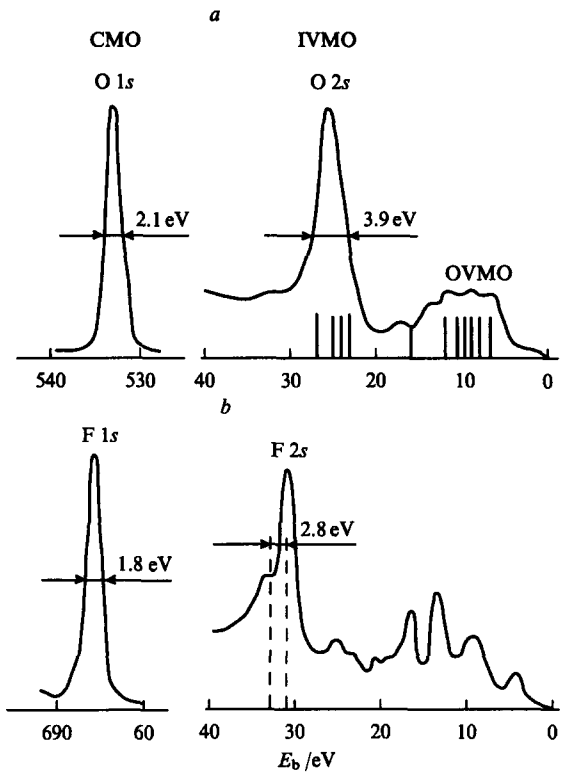


Figure 10. The X-ray photoelectron spectra of SiO_2 (*a*) and the manganese organometallic compound $[CpMn(CO)_2NO]^+PF_6^-$ (*b*). Vertical lines show the theoretically predicted spectra of the outer electrons.[17]

c. Lanthanide compounds

With all other conditions satisfied IVMO formation also requires that the energies of the corresponding occupied AOs of neighbouring atoms are comparable.[21] In this connection, lanthanide compounds are of great interest since the energies of Ln 5*p* (where Ln designates a lanthanide element) and O (F) 2*s* orbitals are close in magnitude. As the atomic number increases from 57 (La) to 71 (Lu), the binding energy of the Ln $5p_{3/2}$ electrons in lanthanide oxides ranges within the limits from 17.7 to 27.5 eV.[19] The binding energies of the O 2*s* electrons (~21 eV) fall approximately in the middle of this interval. All lanthanide oxides from La to Lu (except for Pm) have been studied by XPS.[19,78–80]

The structures of the oxides vary in a series, and, in certain cases, the oxidation states of metal atoms vary too. Therefore, two sets of isostructural lanthanide compounds, *viz.* *o*-methoxybenzoates and diphenylacetates, have been studied (for all but promethium compounds) to solve the problem of IVMO formation (Fig. 11).[19] These compounds are non-hygroscopic, stable in high vacuum, and insensitive to exciting X-ray radiation. Therefore one could expect that the compounds considered do not undergo structural changes and decomposition during the spectra collection.

Together with the expected separate peaks of Ln $5p_{3/2,1/2}$ and O 2*s* electrons, a fine structure is observed in the region of the binding energies of Ln 5*p* and O 2*s* electrons in the X-ray photoelectron spectra of all the compounds studied (Fig. 11). The most complex fine structures are observed in the mid-row lanthanide oxides since in this case the Ln 5*p* and O 2*s* AOs are closest in energy.[4,5] Theoretical calculations for various Ln–O bond lengths have been performed for clusters LnO_7^{11-} and LnO_6^{9-} of C_{3v} and D_{3d} symmetry types respectively at the SCF Xα-DV level and for a cluster LnO_3^{3-} of D_{3h} symmetry type at the SCF Xα-SW level of theory. The results obtained support the assumption that the fine structure in the spectra of lanthanide compounds is partly associated with interaction of the Ln 5*p* and O 2*s* shells resulting in

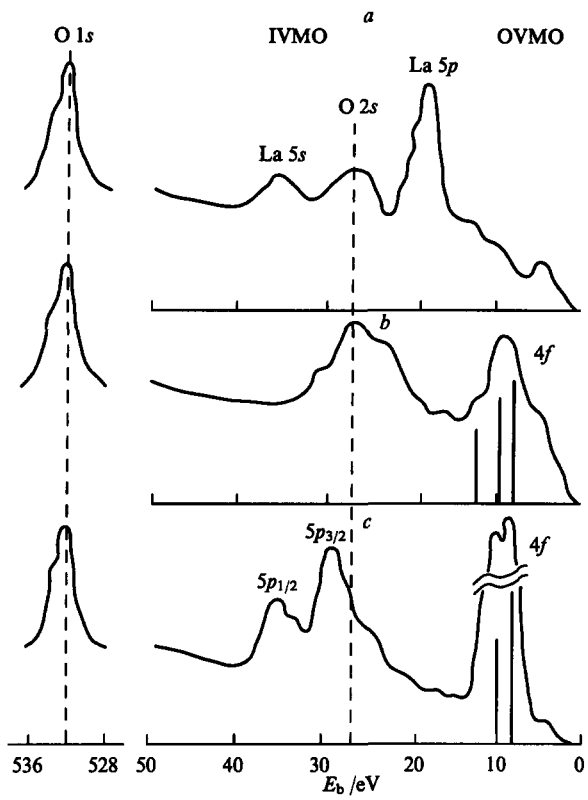


Figure 11. The X-ray photoelectron spectra of La (*a*), Eu (*b*), and Lu (*c*) (LnL_3) *o*-methylbenzoates. Vertical lines represent the theoretical metal 4*f* spectra.[4]

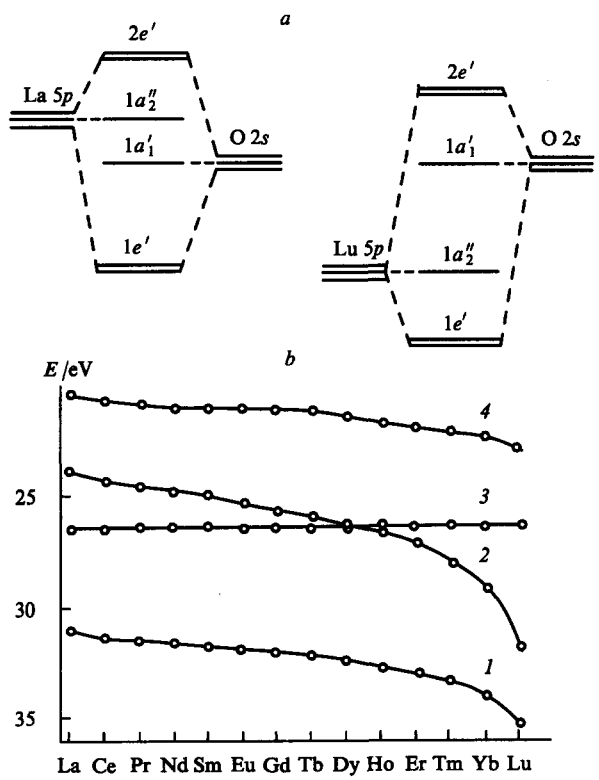


Figure 12. The IVMO diagram (*a*), dependence of the energies of the IVMOs, which consist of the Ln 5*p* and O 2*s* AOs, on the atomic number of the lanthanide element (*b*) for the cluster LnO_3^{3-} (symmetry group D_{3h}).[4] (*1*) $1e'$, (*2*) $1a_2''$, (*3*) $1a_1'$, (*4*) $2e'$.

IVMO formation (Fig. 12). However, the calculations[4] performed do not take into account the relativistic effects, and the cluster LnO_3^{3-} does not exactly represent the structure of the oxygen-containing compounds under consideration. Therefore, a direct, quantitative comparison of the theoretical and experimental results is not possible. However, the very fact of IVMO formation can be proved by the calculation results.

Spectra of lanthanide fluorides also exhibit fine structure in the region of F 2*s* electrons.[19,82] These structures cannot be attributed to the presence of fluorine atoms in different oxidation states since only one relatively narrow peak corresponds to the F 1*s* electrons in the X-ray photoelectron spectrum. It was therefore assumed that the structure observed is concerned with the IVMO electrons.[19,82] The results of the SCF Xα-DV calculation[95] of the electronic structure for cluster LaF_{11}^{8-} of D_{3h} symmetry group agree qualitatively with these experimental data.

d. Actinide compounds

In XPS studies of actinide compounds, much attention has been paid to uranium compounds. It is on the basis of their X-ray photoelectron spectra that the most interesting conclusions on the role of the An 5*f* electrons (where An is a actinide element) in chemical bonding in actinide compounds[96] and on the contribution of the low-energy filled subshells to the bonding have been derived.[2,3,6,18,78]

It is most convenient to consider the participation of the U 5*f* electrons in chemical bonding with stable uranium oxides as an example. Uranium dioxide UO_2 has a fluorite-type (CaF_2) structure, while the trioxide UO_3 is built up of planar networks of tetragons centered with nearly linear uranyl UO_2^{2+} fragments.[18] This fragment serves as a basis for many oxygen-containing uranium compounds with various ligands in its equatorial plane. Special attention is drawn to the low-energy part of the X-ray photoelectron spectra of these compounds.

A high extent of localisation of the non-bonding U 5*f* electrons on the uranium atoms in UO_2 has been suggested from a neutron diffraction study.[97] The electronic configuration of the U atom in UO_2 is {Rn} $5f^2$, where {Rn} is that of the Rn atom in the ground state. This conclusion has been corroborated with XPS[18,96] and theoretical studies.[3,31,54]

A rather narrow peak corresponding to the U 5*f* electrons is found near the Fermi level in the X-ray photoelectron spectrum of UO_2 (Fig. 13 *a*). This peak is absent in the spectrum of γ-UO_3, but, instead of separate peaks of the U $6p_{3/2,1/2}$ and O 2*s* electrons, a fine structure is observed in the region of the U 6*p* and O 2*s* electrons. Binding energies of the electrons that account for different components of the spectrum change with variation in the U–O bond length in the UO_2^{2+} fragment of various compounds. In particular, the difference in energies between the components in the U $6p_{3/2}$ region of the spectra is the most convenient for measurements. This difference may serve as a measure of the bond length R_{U-O} in the UO_2^{2+} fragment of various compounds.[2,3,6,14,18,76,85]

The X-ray photoelectron spectra of UO_2, UF_4, and other non-uranyl compounds do not exhibit such a complex structure in the region of the U $6p_{3/2}$ electrons. Therefore, the fine structure observed in this spectral interval cannot be attributed to the dynamic effect.[18] Also, the most intense peak of this structure cannot be explained by multielectron excitation. The latter give rise to so-called 'shake-up' satellites of relative intensity of ~20% with respect to that of the major peaks in the spectra of inner electrons. The structures of the low-energy part of X-ray photoelectron spectra of uranyl-containing compounds differ essentially in relative intensities of the constituent peaks, their energy distribution, and relative distances from the structure associated with multielectron excitation and observed in the inner electron spectra of these compounds.[78] The presence of two components in the U $6p_{1/2}$ and O 2*s* region of the spectrum of γ-UO_3 (see Fig. 13) is not consistent with the splitting of the U $6p_{3/2}$ component in the crystal field.[14]

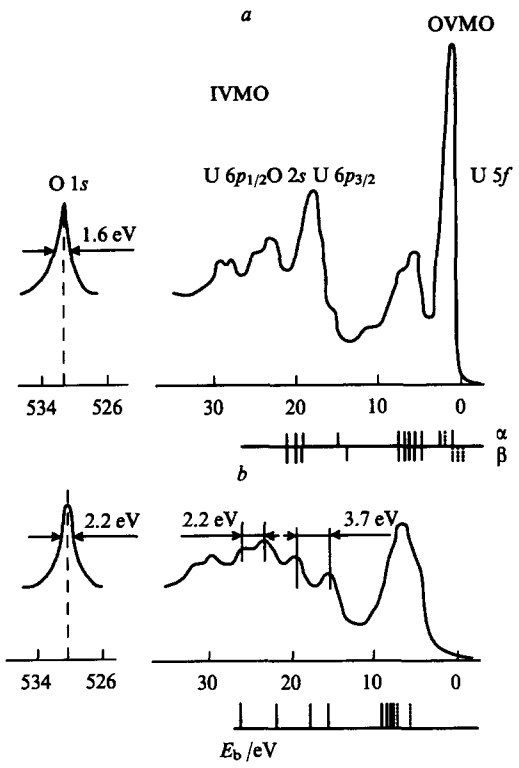


Figure 13. The X-ray photoelectron spectra of uranium oxides UO_2 (*a*) and γ-UO_3 (*b*) and the corresponding energy levels calculated at the SCF Xα-SW level of theory.[3]

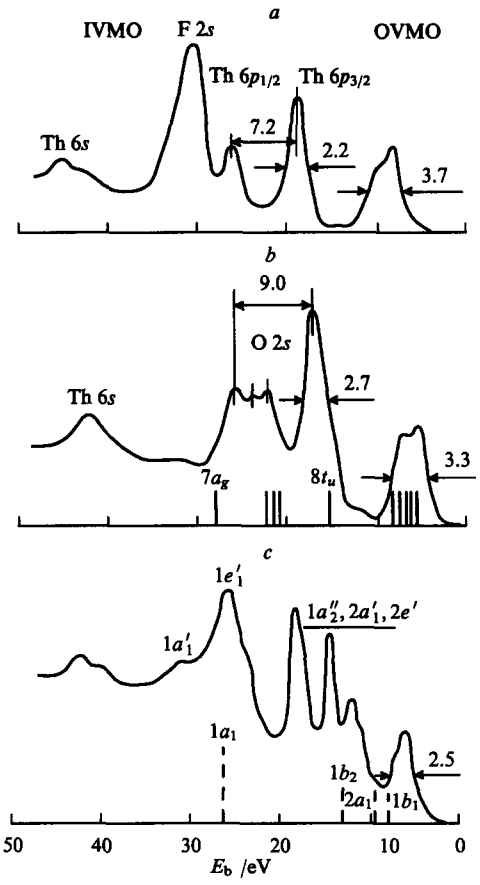


Figure 14. The X-ray photoelectron spectra of weakly-bound Th electrons in ThF_4 (*a*), ThO_2 (*b*)[81] (solid vertical lines represent the electron energies for the cluster ThO_8^{12-} of the O_h symmetry),[54] thorium nitrate (*c*) (dashed lines represent the experimental spectrum of H_2O.[1] The designation of the molecular orbitals of NO_3^- (D_{3h} symmetry group) are shown at the top).

Experimental data[2,3,6,78,83] and the results of theoretical studies performed within the framework of the SCF Xα-SW[3,29] and SCF Xα-DV[30] approaches demonstrate that the complex structure in the U 6*p* and O 2*s* region of the spectra is concerned with the IVMOs that comprise U 6*s*, U 6*p*, and O 2*s* AOs.

The spin-orbit splitting energies of the U 6*p* and Th 6*p* levels differ for the corresponding fluorides, oxides and pure metals (Table 2).[98-101] The variation in the splitting of the level under discussion for Th and its compounds is not attributed to a coincidence of the Th 6*p* peaks and neighbouring ligand peaks since the effect should be reversed in that case (Fig. 14). The

Table 2. The binding energy difference ΔE_b between subshells in Th, U, and their compounds.[76]

Metal or compound	ΔE_b /eV[a]						Ref.
	$6p_{3/2}-6p_{1/2}$	$6p_{3/2}-6s_{1/2}$	$6p_{3/2}-4f_{1/2}$	$6s_{1/2}-4f_{7/2}$	$5d_{5/2}-4f_{7/2}$	X $2s_{1/2}$–X $1s_{1/2}$	
ThO_2	9.0	25.4	317.8	292.4	248.0	508.2	17
	8.5	–	317.6	–	247.9	508.0	98
ThF_4	7.2	26.1	318.2	291.1	248.1	655.7	17
$Th(NO_3)_4 \cdot 4H_2O$	–	25.3	317.4	292.1	248.0	506.6	17
Th	7.5	–	316.6	–	247.6	–	17
	7.9	24.8	316.5	291.7	247.7	–	98
Th_{theor}	9.2	28.7	318.8	290.1	248.0	–	99
UO_2	10.5	27.6, 29.4	362.5	335.3, 333.5	283.6 –	507.2 –	17
	10.6	27.8	362.5	334.7	283.8	507.9	98
UF_4	–	28.2	362.6	334.4	283.6	655.7	17
	11.7	–	362.8	–	–	655.4	100
U	10.0	–	360.6	–	283.0	–	17
	10.0	27.1	360.6	333.5	283.2	–	78
U_{theor}	10.4	31.0	360.9	329.9	283.0	–	79
γ-UO_3	–	–	363.0, 366.7	–	284.0	505.9, 508.1	17

[a] $\Delta E_b = E_b Mn_i l_i j_i - E_b Mn_k l_k j_k$.

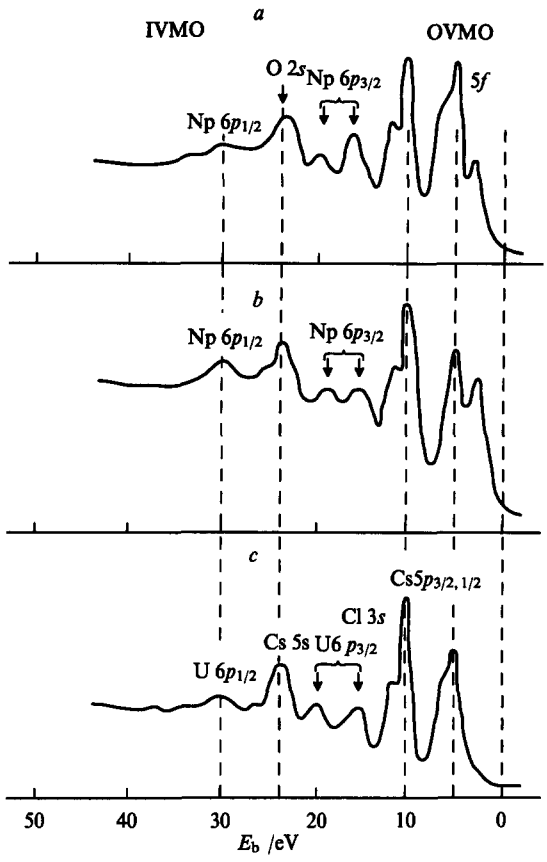


Figure 15. The X-ray photoelectron spectra of weakly-bound electrons of $Cs_2NpO_2Cl_4$ (*a*), $Cs_3NpO_2Cl_4$ (*b*), and $Cs_2UO_2Cl_4$ (*c*) single crystals.[103]

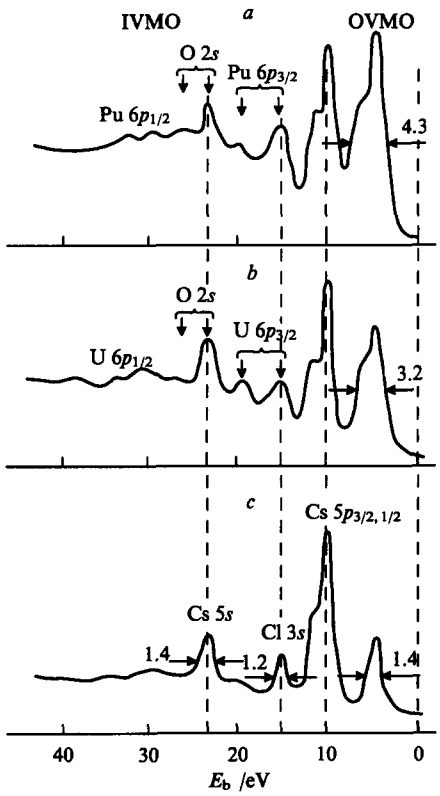


Figure 16. The X-ray photoelectron spectra of weakly-bound electrons of $Cs_2PuO_2Cl_4$ (*a*), $Cs_2UO_2Cl_4$ (*b*), and CsCl (*c*) single crystals.[103]

multiplet splitting effect also does not account for this splitting as long as these compounds are diamagnetic. Extensive experimental data [1-8] show that spin-orbit splitting of inner levels of metal ions depends slightly on the properties of their ligand environment. With this in mind, it was suggested that electrons of the low-energy subshells of Th and U are affected by the chemical bonding in these compounds and take part in IVMO formation.

It is evident from general considerations that, for example, IVMO formation by the Th(U) 6*p* and O 2*s* AOs lowers the binding energy of the Th(U) $6p_{3/2}$ state, etc. It has been mentioned [18] that other effects that shift the energy of low-energy AOs can affect MO formation. Such shifts can be most rigorously detected if the difference in binding energy between the inner valence electrons and deep-lying electrons of core atomic shells in Th and U and their compounds is considered (Table 2). These data accord with the participation of at least Th(U) $6p_{3/2}$ electrons in chemical bonding in the compounds under discussion.

The binding energy difference between the Th $5d_{5/2}$ and $4f_{7/2}$ inner atomic levels is the same for thorium and its compounds within the standard error of measurement. Thus, the essentially increased energy difference between the Th(U) $6p_{3/2}$ and Th(U) $4f_{7/2}$ electrons in Th compounds compared to that in Th metal is a fairly reliable criterion of the contribution of the Th(U) $6p_{3/2}$ and F(O) 2*s* electrons to the chemical bonding in thorium (uranium) oxides and fluorides.[81,101] It has been noted [18] that this difference can be measured most accurately since the corresponding peaks are relatively narrow and hardly overlap with other peaks. Calculations have confirmed a significant participation of the fully occupied Th(U) 6*p* and O 2*s* AOs in the formation of IVMOs in uranium and thorium dioxides.[31,54]

To establish experimentally the formation of IVMOs by An 6*p* and O 2*s* AOs in compounds containing AnO_2^{2+} groups, a series of isostructural single crystals of U, Np, and Pu compounds ($Cs_2UO_2Cl_4$, $Cs_3NpO_2Cl_4$, $Cs_2NpO_2Cl_4$, $Cs_2PuO_2Cl_4$) and polycrystalline samples of Np compounds ($Cs_2NpO_2(CH_3COO)_3$, $RbNpO_2(NO_3)_2 \cdot 2H_2O$, $NaNpO_2(CH_3COO)_3$)[102-104] have been studied by XPS. From analysis of the spectra of the low-energy and inner electrons of these compounds in the X-ray photoelectron spectra of the corresponding oxides and cesium chloride as well as the photoionisation cross-section,[105] it has been concluded [102-104] that IVMOs form in the compounds of Np and Pu considered as well as in uranyl compounds. The inner valence electrons account for the fine structure in the low-energy region of the X-ray photoelectron spectra of these species (Figs 15 and 16). These results are in satisfactory agreement with the results of electronic structure calculations for clusters AnO_2^{2+} (An = U, Np, Pu) of $D_{\infty h}$ symmetry within the framework of non-relativistic SCF Xα-SW [104,106] and relativistic [107,108] approaches as well as clusters $AnO_2Cl_4^{2-}$ (An = U, Np, Pu) at the relativistic Xα-DV level of theory.[111] The structure of the X-ray photoelectron spectra of the 'new product' from the Chernobyl nuclear plant [109] and americium nitrate [110] are also consistent with these results.

It follows from the examples considered in this Section that IVMOs form effectively in compounds of any elements of the Periodic Table if certain conditions are satisfied.

2. Relationship between the structures of compounds and the structures of their X-ray photoelectron spectra

The interpretation of fine structure in an X-ray photoelectron spectrum concerned with IVMOs often utilises not only experimental data, but also results of rather tedious and complicated calculations of the electronic structure of the compound within the framework of the Xα- and other methods that require powerful hardware.[32,106-108] However, the correct model cluster cannot be always chosen at once. In some cases, only approximate data on the structure of the compound are available (especially for amorphous ones). All these factors increase the CPU time required to execute the calculations of the electronic structure. Therefore, qualitative information on the structure of the com-

pound under study obtained from its spectrum is rather helpful, e.g. see Ref. 109.

Several reasons account for the importance of this information. First, reliable information defines a range of species where the formation of IVMOs is expected, thus more precise laborious calculations can be accomplished for them in order to examine the contribution of the IVMO electrons to the chemical bonding. Second, this is useful when relativistic effects are to be taken into account in the interpretation of the spectrum. Third, a possible qualitative interpretation of fine structure in X-ray photoelectron spectra extends the scope of X-ray photoelectron spectroscopy for applied studies of the physicochemical properties of matter.[6, 78, 109]

From the standpoint of group theory, it is expected that fine structure in an X-ray photoelectron spectrum attributed to the IVMO electrons reflects the local environment of the specified atom. The structure of the X-ray photoelectron spectrum is determined by the symmetry point group of the cluster comprising the central atom and the ligands from the closest coordination shells. It is also obvious that the distance between the peaks corresponding to the electrons of different IVMOs must depend on the bond lengths in the cluster. If the IVMO-associated structure in the spectrum is pronounced, then the relative positions of the ligands with respect to the central atom can be easily determined.[17, 20, 78] Estimation of the contribution of the electrons of the inner closed shells to chemical bonding can also be performed. With an experimental or theoretically predicted correlation of the binding energy of the IVMO electrons with the bond lengths in the specified cluster, e.g., UO_2^{2+}, available, the bond lengths in the UO_2^{2+} fragment in any compound or on a solid surface can be determined.[18] It has been mentioned[20, 85] that information of this kind for amorphous compounds cannot be obtained with the same ease since X-ray diffraction cannot be applied for bond length determination in them. Thus, if bond lengths in a cluster have not been determined, then the calculation should be carried out for a certain range of expected distances. We shall consider these points with examples.[1, 17–20, 78]

As has been mentioned above (see Section IV.1), the simplest fine structure is observed in the spectra of diatomic molecules N_2, O_2, F_2, and I_2 (Fig. 7). Two filled ns AOs form two IVMOs, one of them, in accordance with conventional quantum-chemical notation for the two-level system, is formally referred to as the bonding $n\sigma_g$ MO, and the other as the antibonding $n\sigma_u^*$ MO.[21] A considerable energy difference between these two IVMOs (18.7 eV in N_2) points to a significant interaction of electrons of doubly-occupied levels. We should note that, up to the present, the maximum reported to date energy difference is that between $n\sigma_u^*$ and $n\sigma_g$ IVMOs observed in the X-ray photoelectron spectrum of N_2.[1, 51, 56] Despite configuration interaction complicating the fine structure in this region of the spectrum,[86, 87] the peaks corresponding to the electrons of these orbitals are easily distinguished from others (Fig. 7).

The interaction between the electrons of subshells of carbon atoms in the planar layers of pyrographite is of more complex character, therefore, the spectrum of C 2s electrons does not exhibit a sharp fine structure associated with a system of IVMOs (Fig. 7 *a*).[25] Nevertheless, the spectrum shows interaction between the C 2*s* electrons of neighbouring atoms. This interaction manifests itself in the appreciable broadening of the valence band[88] compared with that in the spectra of weakly-bound electrons in solid Si, Ge, and Sn possessing analogous structures.[17]

Fine structures are observed in the *ns* region of the spectra of solid P, As, Sb, and Bi (the electronic configuration of atoms is $\{ns^2np^3\}$)[72] as well as in solid S, Se, and Te (the atomic electronic configuration is $\{ns^2np^4\}$) (Figs 8 and 9).[52] It is known that, in solid sulfur, atoms are arranged in 8-membered twisted rings, and, in solid Se and Te, atoms form linear zigzag chains.[52, 72] A diagram of the energies of IVMOs consisting of the occupied *ns* AOs versus the number of atoms in a planar closed ring or linear chain has been constructed (Fig. 17).[52] These models are closely related to

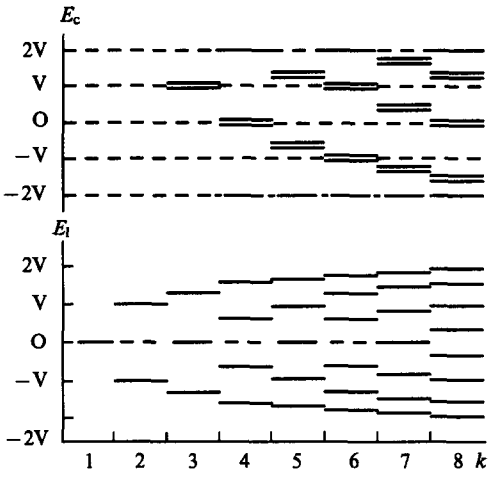


Figure 17. Dependence of the IVMO diagram on the number of atoms in a molecular system (E_c denotes the energy of the ring system, E_l the energy of the linear system, V a relative (Hückel) energy unit).[52]

the real picture. The number of fully-occupied IVMOs increases with the number of atoms k in the ring. The closest agreement between the theoretical and experimental spectra of S 3*s* electrons is reached at $k = 8$. The spectrum considered comprises five peaks in a 1:2:2:2:1 ratio which agrees satisfactorily with the experimental data (see Fig. 9). The linear-chain model does not explain the structure of the spectrum of S 3*s* electrons in solid sulfur. At the same time the predicted and experimental spectra of Se 4*s* and Te 5*s* electrons best fit a linear model with small even k (see Figs. 9 and 17).[52] The Se 4*s* and Te 5*s* spectra of ion-bombarded surfaces of solid Se and Te reveal a single relatively narrow peak[17, 52] with the concurrent disappearance of two peaks, which indicates atomisation of Se and Te on the samples' surface, i.e. the weakening of chemical bonding between neighbouring atoms. This phenomenon may be useful for practical study of radiation-induced damage and defects.

A dependence between the difference ΔE_b in binding energies of the IVMO electrons and the bond length R_{X-X} in solid Se, Te, As, Bi, etc. has been revealed (Fig. 18). A linear correlation of ΔE_b with R_{X-X} suggested previously[11] has a purely illustrative significance.

In transition 3*d* metal disulfides and diselenides, the sulfur and selenium atoms form clusters X_2^{2-} with a marked interaction between the X *ns* electrons of neighbouring atoms.[16] Two peaks associated with electrons of IVMOs are therefore present in the S 3*s* and Se 4*s* X-ray photoelectron spectra.[16] An analogous phenomenon is observed in the X-ray photoelectron spectrum of CuP_2, where, instead of a single peak, two peaks separated by ~4.5 eV are present in the P 3*s* region of the spectrum. It has been noted[16] that these two peaks are concerned with the interaction of P 3*s* orbitals. For the S_2^{2-} cluster, a qualitative agreement between the theoretical and experimental dependences between the binding energy difference ΔE_b of inner valence electrons and the bond length R_{S-S} has been found (Fig. 19). The theoretical dependence obtained within the framework of the CNDO/2 method[17] differs by about 3 eV from the experimental one.

Cluster models can be used to illustrate the correlation of the energy and structure of IVMOs in lanthanide compounds with the structure of the local environment of the metal atom and the distances R_{Ln-X} to the nearest atoms. Within the non-relativistic approximation for the cluster LnO_3^{3-} of D_{3h} symmetry, the IVMO spectrum associated with the Ln 5*p* and O 2*s* AOs corresponds to four energy levels. The highest and lowest ones are the two-fold degenerate $1e'$ and $2e'$ IVMOs, and the two others are the quasi-atomic $1a_1''$ and $1a_2''$ IVMOs (Fig. 12 *a*).[4] The energies of the $1e'$ and $2e'$ MOs must depend on the bond length R_{Ln-O} to a greater extent than those of the $1a_1''$ and $1a_2''$ MOs. The dependence of the

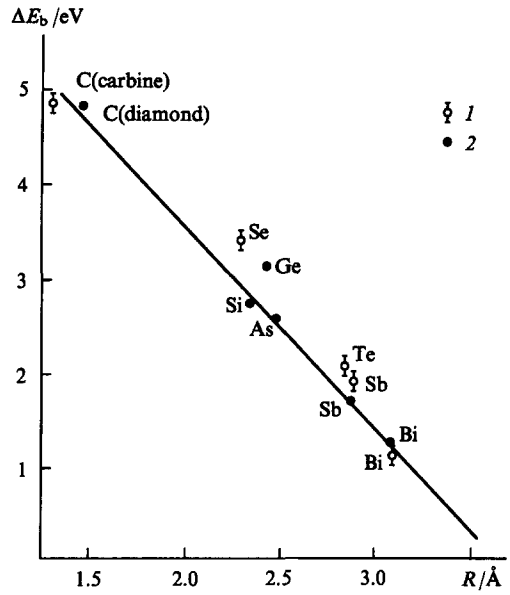


Figure 18. Dependence of the energy gap ΔE_b between the IVMOs, which consist of the *ns* AOs, in solids on the bond lengths *R*. An equation $\Delta E_b = 8.0-2.2R$ is in qualitative agreement with results of studies described in Refs 52, 72 (*1*) and Ref. 11 (*2*).

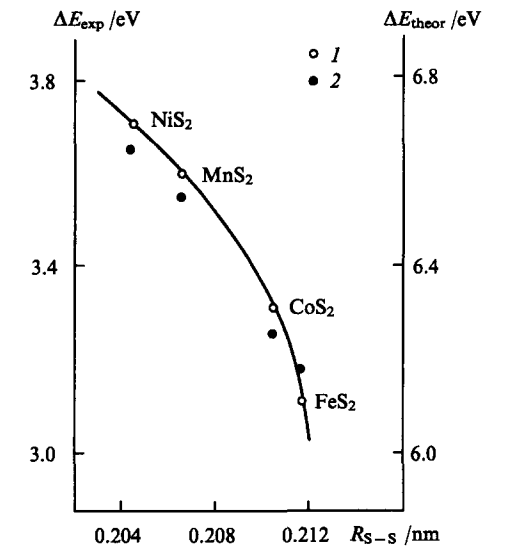


Figure 19. Dependence of the binding energy difference between the $3\sigma_u^*$ and $3\sigma_g$ IVMOs associated with the S 3*s* AOs on the bond length R_{S-S} in the S_2^{2-} cluster of the 3*d* transition metal disulfides: (*1*) experiment;[16] (*2*) theoretical results.[52]

energies of these MOs on the atomic number Z of the central 4*f* element has been calculated for various R_{Ln-O} values at the SCF Xα-SW level of theory (Fig. 12*b*).[4] The energy was calibrated with respect to the energy of the quasiatomic $1a_1'$ IVMO associated mainly with the O 2*s* AO.

The structure of IVMOs for cluster LnO_3^{3-} obtained in terms of group theory is in qualitative agreement with computational results.[4] The IVMO structure for clusters LnO_7^{11-} (symmetry group C_{3v}) and LnO_6^{9-} (symmetry group D_{3d}) is different.[78-80] Electronic structure calculations for lanthanide compounds within the relativistic approach would enable more precise quantitative comparison of theoretical and experimental data.

Oxygen-containing actinide series compounds are the species structural information on which, namely the structure of the local environment of the metal atom and its oxidation state, can be determined from the fine structure corresponding to electrons of IVMOs in their X-ray photoelectron spectra.[3,6,17,18,85,106,107,111] Most clearly this can be illustrated with the spectra of uranium compounds. The results of calculations demonstrate that taking into account the relativistic effects leads essentially to the strong splitting of the U $6p_{1/2}$ component of the doublet and hardly affects the energy of the U $6p_{3/2}$ electrons.[31] Thus, the interpretation of the spectrum in the region of the U $6p_{3/2}$ and O 2*s* electrons can be carried out within the non-relativistic approach.[3]

Substantially different structures of uranium dioxide and trioxide give rise to a fundamental distinction in the spectra of weakly-bound electrons (Fig. 13). Since the U–O bond in the UO_2^{2+} fragment of UO_3 is much shorter than the equatorial U–O bonds, in the first approximation, the structure of the valence region of the spectra is determined by this fragment. It has been mentioned[6,85] that, within the non-relativistic approximation, the correlation diagram of IVMOs consisting of the U 6*s*, U 6*p*, and O 2*s* AOs makes it possible not only to rationalise the structure of the spectra of the uranium oxides under discussion, it can also be helpful in the investigation of the structures of these compounds (Fig. 20).[6,85] According to this scheme, variations in the U–O bond lengths in clusters UO_8^{12-} and UO_2^{2+} slightly influence the energies of the quasi-atomic t_{2g}, t_{2e} (in UO_8^{12-}), and π_u (in UO_2^{2+}) MOs, but can have a substantial effect on the t_{1u}, t_{1u}^* (in UO_8^{12-}), σ_u, σ_u^*, σ_g, and σ_g^* (in UO_2^{2+}) IVMOs. In practice, this phenomenon permits the determination of the structures of oxides and the bond lengths in them.

However, this diagram does not describe completely the structure observed in the spectrum of γ-UO_3.[2,3,6] It is concerned with the fact that it does not take into account the influence of the ligands in the equatorial plane of the UO_2^{2+} fragment on the spectra of the valence electrons of oxygen. Apparently, this

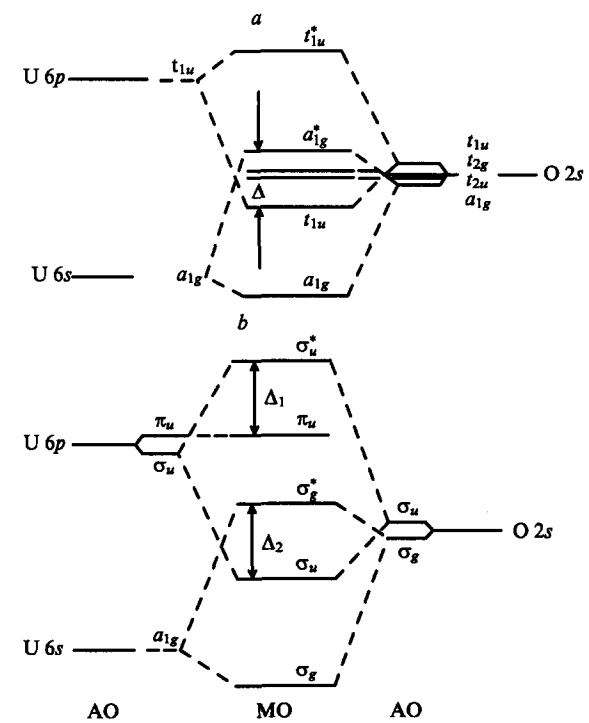


Figure 20. The diagram of IVMOs attributed to the interaction of the U 6*p* and O 2*s* AOs for clusters UO_8^{12-} (*a*) (O_h symmetry group) and UO_2^{2+} (*b*) ($D_{\infty h}$ symmetry group).[6,85]

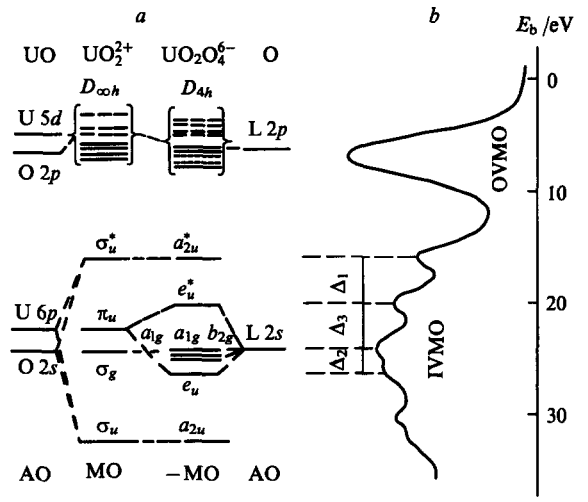


Figure 21. The principal scheme for MO formation in clusters UO_2^{2+} ($D_{\infty h}$ symmetry group) and $UO_2O_4^{6-}$ (D_{4h} symmetry group) (*a*) and the X-ray photoelectron spectrum of γ-UO_3 (*b*).[106]

influence gives rise to additional IVMOs consisting of the U 6*p* and O 2*s* AOs. In the scheme, which accounts for the effect of the equatorial ligands on the structure of IVMOs of the UO_2^{2+} ion, these MOs correpond to the $^*e_u$ and e_u^* orbitals (Fig. 21).[106] The latter scheme almost completely describes qualitatively the structure of the valence electron region of uranyl compounds. The results of theoretical calculations for clusters of uranyl compounds,[3,106] which take into account the effect of the equatorial ligands are consistent with the results obtained from this scheme.

Thus, the experimental correlation of the energy gap between the two components in the U $6p_{3/2}$ region of the spectrum (in Fig. 20, they are related to the a_{2u}^* and e_u^* IVMOs) with the U−O bond length in the UO_2^{2+} fragment in a series of uranyl compounds becomes comprehensible.[17,85] The results of semiempirical calculations[106] of structural characteristics of clusters $UO_2L_n^{m-}$ are consistent with this dependence. In certain cases, the phase content of natural uranium oxides and some bond lengths in them have been determined from these data.[2,6,17,85] The correlation of the structure of a compound with the fine structure in the X-ray photoelectron spectra of the valence region has also been studied in a series of Np, Pu (Figs 15 and 16),[102-104] and Am[110] compounds.

Since ThO_2 and UO_2 have similar structures,[17] their spectra (Figs 13 and 14) have much in common (see Fig. 20). Thus, in the O 2s region, the structure associated with the t_{1u} IVMO is observed. In the Th $6p_{1/2}$ region of the X-ray photoelectron spectrum of $Th(NO_3)_4 \cdot 4H_4O$, peaks corresponding to the $1a_1'$ and $1e_1'$ IVMOs of the NO_3^- cluster are present.[81]

In many cases, the fact of the formation of IVMOs in various compounds can be authenticated by the presence of fine structure in the region of weakly-bound electrons in their X-ray photoelectron spectra. This structure can often be interpreted without recourse to rigorous theoretical calculations by a simple approach based on group theory.[17,20,78] A correlation of the structure of a compound, i.e., bond lengths, with the structure of their spectra associated with the inner valence electrons has been established. It allows in some cases the retrieval of qualitative and quantitative information on the structure of compounds, which is exceptionally important for amorphous materials.

V. Contribution of inner valence molecular orbitals to chemical bonding

From the viewpoint of quantum-chemical theory, provided certain conditions are satisfied, MOs can be formed from arbitrary low-lying filled AOs.[21,22] The contribution of electrons to the chemical bonding is defined with a specific model describing the bond formation. The chemical bonding in homonuclear molecules is assumed to occur essentially due to the electrons of valence atomic shells,[21,22] and the electrons of inner closed shells contribute to the chemical bonding to a lesser extent and destabilise the bonds. Thus, in a molecule A_2, two occupied 1*s* AOs can form a bonding $1\sigma_g$ and antibonding $1\sigma_u^*$ MOs. The bonding MO stabilises the bond to a lesser degree than the antibonding one destabilises it.[21] Therefore, the total contribution of the CMO electrons to the covalent component of the bond energy is negative. In particular, this explains the instability of the helium molecule He_2.[21]

However, as follows from experimental data on light-element compounds, both filled and valence shells with the same principal quantum number contribute to the chemical bonding.[1] Calculations of the electronic structure of light-element diatomic molecules within the MO LCAO approach have indicated that the occupied low-energy AOs do not form 'pure' CMOs but mix with valence AOs.[1,51,52,56,73,88] These CMOs lose their 'inner' character and have to be considered collectively with the OVMOs. They are referred to as IVMOs since they have not fully become the valence ones.[51,56]

The question of the participation of the electrons of filled low-energy shells in chemical bonding for light-element compounds has been considered to some extent. However, it had barely been raised for heavy-element compounds until recently.[17,85] Consider, for example, an established fact of the formation of IVMOs in uranyl compounds by the U 6*p* and O 2*s* AOs.[2,3,6] If these MOs consisted solely of the U 6*p* and O 2*s* AOs, they would not be referred to as valence MOs. However, they were given the name 'IVMO' since they also consist of the valence U 7*s*, 6*d*, 4*f*, and O 2*p* AOs.

The question of the role of the low-energy closed shells of heavy elements (lanthanide compounds, actinide compounds,etc.) in chemical bonding raised on the basis of XPS studies[2-6,26,27,78] is very important. Its examination will help in understanding the nature of chemical bonding in these compounds, furnish an explanation of the existence of unique nearly linear stable fragments, AnO_2^{n+}, in certain actinide compounds, etc. However, difficulty in rigorous theoretical calculations for actinide series compounds is now evident. Therefore, as has been mentioned,[17,20] the first step is to consider the participation of inner electrons in chemical bonding for the most simple molecules,[51-53,56,71,73-75,88] and then to proceed to heavy-element compounds.

1. Simple models

Examination of correlations of MO energies with interatomic distances can help understanding of the formation of these MOs.[3,4,51-53,56,72,73,85,112] The N_2 molecule is the most convenient subject for examination of this kind. Calculations of the MO energies for N_2 at different interatomic distances were carried out at the SCF CNDO/2 and SCF Xα-DV levels (Fig. 22).[51,56] The results obtained by these two approaches are in good conformity with each other. They display the same trend of changes in the orbital energies with decrease in the bond length and the same order of MO energies at the equilibrium interatomic distance $R_e = 0.109$ nm. They also give comparable values of the binding energy gap between electrons of the bonding $2\sigma_g$ and antibonding $2\sigma_u^*$ IVMOs.

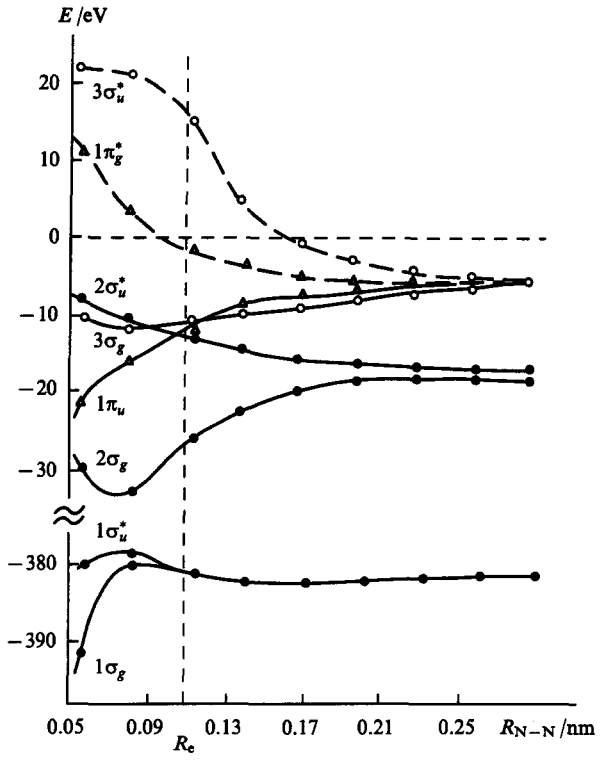


Figure 22. The SCF Xα-DV orbital energies of N_2 as functions of the bond length R_{N-N} (R_e is the equilibrium distance).[51,56]

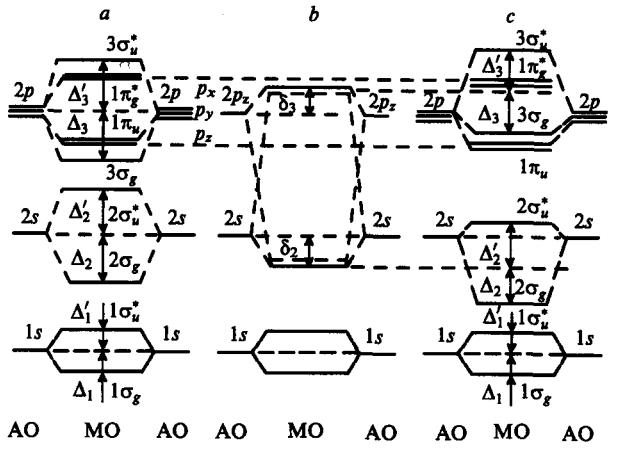


Figure 23. Scheme of formation of OVMOs, IVMOs, and CMOs in a nitrogen molecule: (*a*) — overlap of 2*s* and 2p_z AOs is neglected; (*b*) — the '*s*–*p*' interaction; (*c*) — with 2*s*–2*p* overlap taken into account.[51,56]

As nitrogen atoms are brought together to the equilibrium distance, not only the orbital energies, but also the order of MO as regards their energies change. This results in the formation of the $1\sigma_g$ and $1\sigma_u^*$ CMOs and $2\sigma_g$ and $2\sigma_u^*$ IVMOs, which, to a substantial degree, are contributed by the N 1*s* and N 2*s* AOs respectively. An increase in the energy of the doubly-degenerate $1\pi_u$ VMO made up of the $2p_x$ and $2p_y$ AOs is greater in magnitude than that of the $3\pi_g$ VMO that is primarily composed of the $2p_z$ AO. It points to a greater contribution of the $1\pi_u$ VMO to the covalent component of the N–N bond compared with that of the $3\sigma_g$ VMO. Weak dependence of the energies of the $2\sigma_u^*$ and $3\sigma_g$ MOs on the interatomic distance ranging from R_e to R = 0.35 nm indicates insignificant values of the corresponding orbital force f_i and thus essentially non-bonding character of the N 1*s* AOs.

In a certain approximation, the contribution of the N 1*s* electrons to the chemical bonding in N_2 can be neglected since the energies of the $1\sigma_g$ and $1\sigma_u^*$ CMOs hardly depend on the interatomic distance within the same interval. As the atoms continue to close with each other, the energy of the $1\pi_u$ VMO increases and that of the $3\sigma_g$ VMO decreases. Such behaviour could be attributed to an increase in the overlap integral of $2p_x$ and $2p_y$ AOs and a decrease in that of $2p_z$ AOs of neighbouring atoms at small *R*. At $R \leqslant R_e$, the energies of the $1\sigma_g$ and $1\sigma_u^*$ CMOs behave like those of the $2\sigma_g$ and $2\sigma_u^*$ IVMOs at $R > R_e$. The energies of the antibonding $1\sigma_u^*$ and $2\sigma_u^*$ MOs depend on the interatomic distance to a lesser extent than the energies of the corresponding bonding $1\sigma_g$ and $2\sigma_g$ MOs.

Changes in orbital energies of N_2 with decreasing bond length can be easily followed in a simple scheme (Fig. 23).[51,56] This scheme may be used for consideration of any homonuclear diatomic molecule formed from *p*-block elements $\{ns^2np^m\}$. An example of a molecule where MOs are formed by individual AOs (the $1\sigma_g$ and $1\sigma_u^*$ CMOs, $2\sigma_g$ and $2\sigma_u^*$ IVMOs, and $3\sigma_g$, $1\pi_u$, $1\pi_g^*$ and $3\sigma_u^*$ VMOs are represented) is shown in Fig. 23 *a*. The value of the splitting $\Delta_i' > \Delta_i$ (i = 1, 2, 3), and $\Delta_+ = \Delta_i + \Delta_i'$ depends on the bond length. Totally occupied CMOs destabilize the bond. Since the difference $\Delta_- = |\Delta_i' - \Delta_i|$ is not too great, decrease of the bond length causes comparable changes in energies of the bonding and antibonding MOs. It is observed for $1\pi_u$ and $1\pi_g^*$ VMOs (Fig. 22). Unlike the π-type MOs, the σ-type MOs are formed by the 2*s* AOs as well as the $2p_z$ AOs. At R_e = 0.109 nm, the 2σ and $2\sigma_u^*$ IVMOs and $3\sigma_g$ VMO consist of the 2*s* and $2p_z$ AOs in 84 : 16, 69 : 31, and 84 : 16 ratios respectively. In Fig. 23 *b*, the formation of the σ-type MO by the $2p_z$ and 2*s* AOs is schematically shown. The magnitude of this '*s*–*p*' interaction also depends on the bond length. Bonding and antibonding MOs shift in opposite diractions to the same extent if the '*s*–*p*' interaction affects them equally (Fig. 23 *b*). In reality, this interaction does not affect each type of MO equally, thus it gives rise to an even more asymmetrical shift of the MO energies from their initial values. With regard to this, with decrease in the bond length in the N_2 molecule, the 'centre of mass' of the σ-type VMOs shifts to a greater extent than that of the IVMOs, i.e., formally, $\delta_3 > \delta_2$ (see Figs 22 and 23). Thus the order of MOs may change, as is observed in the $1\pi_u$–$3\sigma_g$ pair of VMOs. Also, the overlap between the $2p_z$ AOs decreases at shorter *R* compared with that of the $2p_x$ and $2p_y$ AOs, and it affects the energies of the $1\pi_u$ and $3\sigma_g$ VMOs.

Despite the formalism of the separation of the total interaction between the electrons of neighbouring atoms, this simple approach, not taking into account atomic *s*–*p* hybridisation, furnishes an explanation of the observed changes in the orbital energies with decrease of the N–N bond length and inversion of the $3\sigma_g$ and $1\pi_u$ MOs. Also, it explains the non-bonding character of the $2\sigma_u^*$ and $3\sigma_g$ MOs and the positive contribution of the $2\sigma_g$ and $2\sigma_u^*$ IVMOs to the bond energy in N_2. Estimation of contributions of individual MOs to the chemical bonding in N_2 within the CNDO/2 approach has been based on analysis of the resonance energy E_{AB}^R (see Eqn 10) that represents the degree of covalence of the bond A–B (Fig. 24).[51,52,56] The contributions of electrons of the $1\sigma_g$ and $1\sigma_u^*$ CMOs to the bond energy were not estimated.

We should mention that the results obtained do not conform to the conventional viewpoint on the character of the chemical bond in N_2.[21,22] To a certain approximation, as before, this bond may be treated as a triple bond, which is not attributed to electrons of the $3\sigma_g$ and $1\pi_u$ OVMOs,[21,22] but to electrons of the $1\pi_u$ OVMO and $2\pi_g$ IVMO. The contribution to the N≡N bonding of electrons of the $2\sigma_g$ IVMO, which primarily consists of N 2*s* AOs, is comparable with that of electrons of the twofold-degenerate $1\pi_u$ OVMO.[51,56]

The F_2 molecule, in which both the antibonding $1\pi_g^*$ and bonding $1\pi_u$ OVMOs are totally-occupied is yet another example of the contribution of the inner valence electrons to the chemical bonding. According to the traditional model of the formation of a

Table 3. Energies of MOs (eV) and their content (%) for different bond lengths R_{F-F} (nm) in F_2 calculated at the CNDO/2 level.[73]

Molecular orbital	$R_1 = 0.05$				$R_e = 0.1417$				$R_2 = 0.20$			
	E_1	2s AO	$2p_z$ AO	$2p_x(2p_y)$ AO	E_e	2s AO	$2p_z$ AO	$2p_x(2p_y)$ AO	E_2	2s AO	$2p_z$ AO	$2p_x(2p_y)$ AO
$3\sigma_u^*$ OVMO	22.83	79	21	–	2.05	5	95	–	−5.91	–	100	–
$1\pi_g^*$ OVMO	−1.00	–	–	100	−22.09	–	–	100	−23.69	–	–	100
$3\sigma_g$ OVMO	−16.13	21	79	–	−22.73	2	98	–	−16.20	–	100	–
$1\pi_u$ OVMO	−46.86	–	–	100	−25.77	–	–	100	−24.17	–	–	100
$2\sigma_u^*$ IVMO	−40.60	39	61	–	−41.99	5	95	–	−44.41	100	–	–
$2\sigma_g$ IVMO	−78.51	90	10	–	−49.74	98	2	–	−45.89	100	–	–

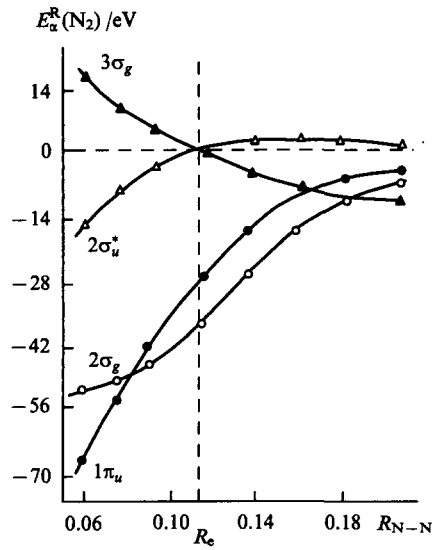


Figure 24. Dependence of E_α^R quantities, which characterise the MO contribution to the covalent bonding, on the bond length R_{N-N} for N_2.[51,56]

chemical bond,[21,22] the contributions of electrons of these OVMOs and of electrons of the bonding $2\pi_g$ and antibonding $2\pi_u^*$ IVMOs are assumed to mutually neutralise. However, this assumption is not valid since the dependence of the MO energies in F_2 on the bond length R_{F-F} (see Ref. 73) points to different orbital forces f_i for the $2\sigma_g$ and $2\sigma_u^*$ IVMOs.

The estimation of the contributions of the electrons of various MOs to the chemical bonding in F_2 within the approach of separation of total energy demonstrates that, at an equilibrium distance R_e, the influence of electrons of the $1\pi_u$ and $1\pi_g^*$ OVMOs compensate each other, and the contribution of electrons of the $2\sigma_g$ IVMO is somewhat greater than that of electrons of the $2\sigma_u^*$ IVMO.[73] As a result, *the covalent component of the F−F bond is* mainly associated with the electrons of the $3\sigma_g$ OVMO and, partly, $2\sigma_g$ IVMO. The latter accounts for 44% of the total covalent component of the bond energy. Thus, the substantial contribution of the IVMOs to the chemical bonding in F_2 is attributed to mixing of fully-occupied and valence AOs (Table 3).

The quantum-chemical estimation of bonding (antibonding) character of MOs for F_2 was also accomplished with the aid of the orbital force f_α approach. The calculation utilised the SCF Xα-SW method with respect to the orbital relaxation within the framework of the transition state principle.[73] The X-ray photoelectron spectrum of the weakly-bound electrons of F_2 has been used for the data interpretation (see Fig. 7).[23] Unlike the Xα-calculation, *ab initio*[113] and semiempirical CNDO/2[73] calculations give the wrong order of the MO energies within the Koopmans's approximation (Table 4): the $3\sigma_g$ OVMO is between two π-type MOs, which does not agree with the order determined experimentally (see Fig. 7). The results obtained at these levels of theory are less precise than those obtained by Xα-methods of calculation. The

Table 4. Vertical ionisation potentials for valence electrons of F_2 at the equilibrium bond length $R_e = 0.1417$ nm.

Calculation method	IP /eV					Ref.
	$1\pi_g^*$ OVMO	$1\pi_u$ OVMO	$3\sigma_g$ OVMO	$2\sigma_u^*$ IVMO	$2\sigma_g$ IVMO	
Experiment	15.9	18.8	21.1	37.5	41.8	23
Ab initio	18.0	21.9	20.3	40.7	47.8	113
Xα-DBM	16.0	18.6	20.8	33.7	39.3	32
CNDO/2	22.1	25.8	22.7	42.0	49.7	73
Xα-SW	16.8	19.5	20.7	34.7	39.5	73

Xα-SW modification is preferable for the interpretation of the binding energies of electrons of IVMOs.

The values of the derivatives E_b' (of the orbital forces f_i) at the equilibrium interatomic distance $R_e = 0.1417$ nm in the F_2 molecule show that the electrons of the $2\sigma_g$ IVMO make the largest contribution to the bonding in the system. The $2\sigma_u^*$ IVMO destabilises the F−F bond, but does not entirely compensate the stabilisation from the $2\sigma_g$ IVMO (Table 5).

Table 5. Orbital forces E_b' for valence orbitals of F_2 at the equilibrium distance $R_e = 0.1417$ nm.[17]

Molecular orbital	E_b' /10^{-8} N per electron,		
	ab initio[a]	CNDO/2	Xα-SW
$1\pi_g^*$ OVMO	−0.93	−0.89	−0.71
$1\pi_u$ OVMO	0.98	0.89	1.79
$3\sigma_g$ OVMO	1.69	1.08	1.43
$2\sigma_u^*$ IVMO	−1.24	−0.96	−1.78
$2\sigma_g$ IVMO	2.42	2.05	2.85

[a] Calculated from cited in Ref. 113 MO energies at two distances R_{F-F} equal to 0.1336 and 0.1417 nm.

In the X-ray photoelectron spectrum of F_2, the peak corresponding to the $2\sigma_g$ electrons is broader than that corresponding to the $2\sigma_u^*$ electrons (their half-widths are 2.7 and 1.6 eV respectively).[23] Several final states of the system after photoemission could account for this distinction. Theoretical calculation in terms of the configuration interaction can corroborate this assumption. A dependence of the gradient of the ionisation potential of these orbitals on the bond length R_{F-F} could be another reason; this is in full agreement with results of the Xα-SW calculation. Actually, the ratio of $2\sigma_u^*$ and $2\sigma_g$ peaks' half-widths is 0.59, while the ratio of the absolute values of the orbital forces f_α is 0.62 (Table 5).

Despite the different profiles assigned to the different contributions of electrons of the $2\sigma_u^*$ and $2\sigma_g$ IVMOs to the chemical bonding in F_2, the integral intensities of these peaks are almost equal,[23] which points to their essentially identical photoionisation cross-sections, and thus to equal 2s character of these IVMOs. The results of the Xα-SW calculation[73] are also consistent with this

Table 6. Energies E_b and distribution of electronic charge Q (%) for valence orbitals of F_2 at the equilibrium distance $R_e = 0.1417$ nm for ground and transition states.[73]

Molecular orbital	E_b /eV	Charge Q in areas			
		atomic		interatomic	outer
		F 2s	F 2p		
Ground state					
$1\pi_g^*$ OVMO	10.50	0	79.2	15.0	5.8
$1\pi_u$-OVMO	13.50	0	70.7	23.1	6.2
$3\sigma_g$-OVMO	14.56	2.2	77.3	11.7	8.8
$2\sigma_u^*$-IVMO	28.31	81.8	2.0	11.1	5.1
$2\sigma_g$-IVMO	33.18	78.3	2.0	17.1	2.6
Transition state					
$1\pi_g^*$-OVMO	16.80	0	80.8	14.4	4.8
$1\pi_u$-OVMO	19.50	0	72.8	22.0	5.2
$3\sigma_g$-OVMO	20.70	2.4	78.5	11.3	7.8
$2\sigma_u^*$-IVMO	34.70	82.7	1.9	10.8	4.6
$2\sigma_g$-IVMO	39.50	79.0	2.0	16.7	2.3

premise (Table 6). Different contributions of the $2\sigma_u^*$ and $2\sigma_g$ IVMOs would imply a significant dependence of the photoionisation cross-sections on the energy of the levels in question, a dependence that is unlikely due to the close binding energies of electrons of the $2\sigma_u^*$ and $2\sigma_g$ IVMOs (see Table 5). It follows from Table 6 that the IVMOs are built up mainly of the F 2s AOs, the contributions of which are nearly the same and change little during the relaxation of the ionised system. An essential contribution of the F 2s AO to the $2\sigma_u^*$ IVMO accounts for the significant stabilisation of this MO, unlike that in N_2 molecule, which is characterised by a greater percentage of the N_2 2p AO.[51,56] The energy gap between the IVMOs in F_2 (4.3 eV, Table 4) is much smaller than the corresponding value (18.7 eV) in N_2.[51,56] Specific characteristics of the IVMO in F_2 also account for a clearly bonding character of the $3\sigma_g$ OVMO (Table 5), as soon as this OVMO consists mainly of the F $2p_\sigma$ AOs (see Table 6).

Analogous results have also been obtained for other diatomic Group IV–VIIA second and third Period molecules and clusters.[17,52,71,72,88]

The same reasoning can be applied to the dependence of the orbital energies of the uranyl fragment UO_2^{2+} on the bond length R_{U-O} obtained within the framework of the SCF Xα-SW approach (Fig. 25).[3,106] The dependence obtained is in a good qualitative agreement with the corresponding data for N_2. As atoms are brought together, the energies of the antibonding $8\sigma_u^*$ (UO_2^{2+}) and $2\sigma_u^*$ (N_2) IVMOs change to a lesser extent than the energies of the corresponding bonding $7\sigma_u$ and $2\sigma_g$ IVMOs, thus a considerable contribution of the $8\sigma_u^*$ and $7\sigma_g$ electrons to the bonding in UO_2^{2+} is suggested. As has already been mentioned for N_2, this effect arises due to the mixing of the valence and doubly-occupied low-energy AOs of adjacent atoms leading to the formation of IVMOs. Apparently, this mixing also accounts for the inversion of the $7\pi_u$, $9\sigma_u$, $4\sigma_g$, and $12\sigma_g$ OVMOs of the uranyl fragment caused by a change in the U–O bond length (Fig. 25). The MO contributions to the chemical bonding were estimated from the values of orbital forces f_i calculated from the E_i *vs.* R_{U-O} dependences.[113] It has been found that, at $R_{U-O} = 0.173$ nm, electrons on IVMOs account for 29% of the total electron contribution in the uranyl cluster.

The calculation of the electronic structure of the uranyl cluster by the SCF Xα-DV method yields similar results (Figs 26 and 27).[77] In Fig. 27, vacant MOs are shown as dashed lines, and occupied MOs as solid lines. Presented in the Figure are the atom content, energies (to the left), and the E_α^R values (to the right), which characterise the contribution of IVMOs to the

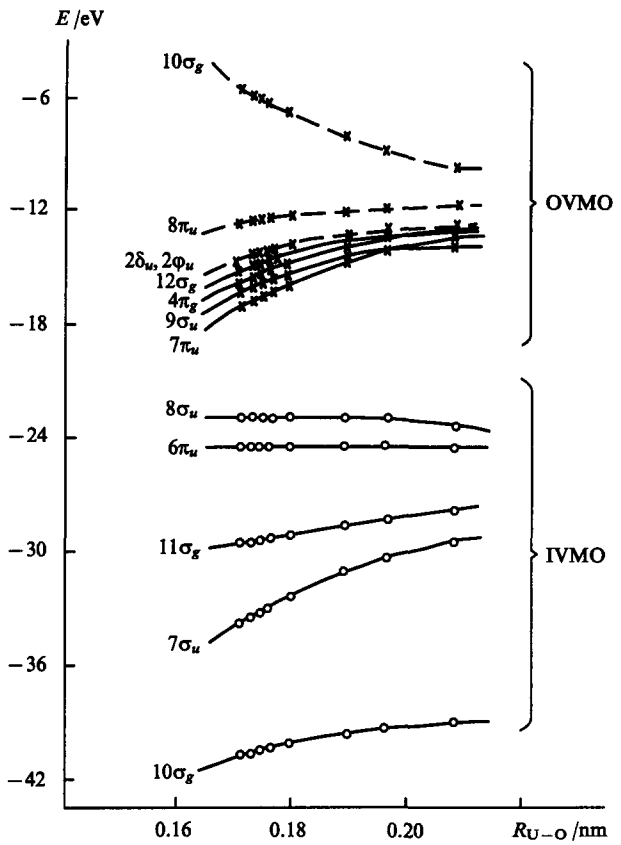


Figure 25. Dependence of the MO energies for the cluster UO_2^{2+} (symmetry group $D_{\infty h}$) on the bond length R_{U-O} calculated in the SCF X_α-SW approach.[106]

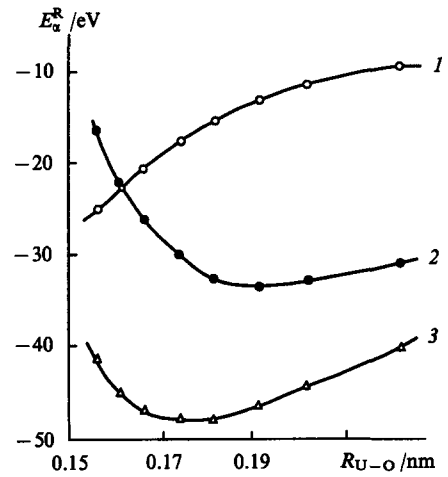


Figure 26. Dependence of the energy contribution of electrons of the IVMOs (*1*), OVMOs (*2*), and of the total electron contribution (*3*) to the covalent bonding E_α^R on the bond length R_{U-O} for UO_2^{2+}.[77]

covalent bonding of the cluster UO_2^{2+}. At $R_{U-O} = 0.173$ nm, the electrons of IVMOs account for 37% of the total electronic contribution in UO_2^{2+}. Similar calculations have also been performed for the cluster $UO_2Cl_4^{2-}$ of D_{4h} symmetry.[17] The contributions of the electrons of OVMOs and IVMOs to the chemical bonding in UO_2^{2+} somewhat depend on the bond lengths R_{U-O} (Fig. 26).

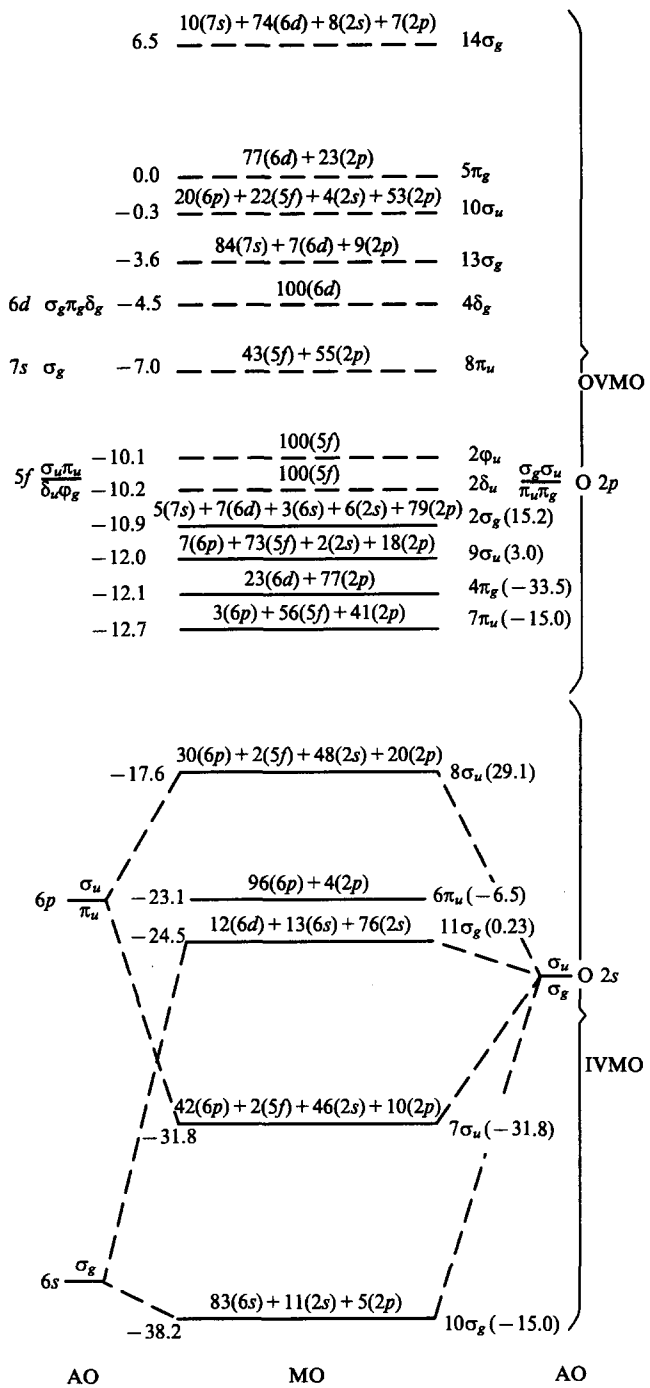


Figure 27. The MO diagram for UO_2^{2+} (symmetry group $D_{\infty h}$) at $R_{U-O} = 0.173$ nm (the SCF Xα-DV method). Energies of MOs (in eV), their content (%), and the values of E_α^R (in eV) characterising the MO contribution to the covalent bonding are displayed in parentheses.[77]

2. Crystal framework

From the data presented above we may assume that the inner valence electrons contribute to the chemical bonding not only in molecules, but also in crystals. In essence, this applies to covalent crystals. To this end, quantum-chemical calculations of the band structure of black phosphorus have been made.[75] The choice of the subject of study is concerned with the monoatomic character of the crystal lattice, which excludes the ionic component of the bonding, the availability of reliable crystallographic data [114] and of X-ray photoelectron spectra obtained with a synchrotron radiation source.[115] The calculations of the band structure of black phosphorus have been carried out by the crystal orbital method within the framework of the extended Hückel method (EHM) by a program described in a previous study.[116]

The crystal lattice of black phosphorus is built up of crimped layers.[114] The unit-cell dimensions *a*, *b*, and *c* are 0.33136, 1.0478, and 0.43763 nm respectively. Each phosphorus atom has three closest neighbours within the layer at a distance of 0.2244, 0.2224, and 0.2224 nm. The layers are separated from each other so that the minimum distance between two phosphorus atoms belonging to adjacent layers is 0.3592 nm. At this distance, the overlap integral between the two atomic Slater 3*s* and 3*p* orbitals, the exponential factors of which have been defined according to Clementi [117] is close to zero. Therefore, the basic aspects of the band structure of black phosphorus can be described satisfactorily within a two-dimensional representation with four atoms per unit cell.

The unit cell of the layer consists of two pairs of phosphorus atoms. The bond axes make an angle of 44.17° with the crystallographic *a* axis.[114] The distance R_{P-P} within pairs is 0.2224 nm, the distance between the axes of pairs along the *c* axis is 0.2130 nm. Translational constants along two perpendicular directions are equal to the values of constants *a* and *c*, respectively.

The two-dimensional Brillouin zone for the layer under consideration is rectangular, its centre is designated as Γ; points *J* and *K* refer to the middle of the longest side and the vertex of the Brillouin zone, respectively. Direction $\Gamma \rightarrow J$ is denoted as Σ_1, $J \rightarrow K$ as Σ_2, and $K \rightarrow \Gamma$ as Σ_3.

The energies of the crystal valence orbitals $E_i(k)$ are determined along these directions and in points Γ, *J*, and *K* from the secular equation:

$$\sum_\nu [F_{\mu\nu}(k) - S_{\mu\nu}(k)E_i(k)]c_{i\nu}(k) = 0\,, \qquad (35)$$

where $F_{\mu\nu}(k)$ and $S_{\mu\nu}(k)$ are matrix elements of the one-electron operator and the overlap integral between the Bloch basis functions, respectively.

For the P 3*s* and 3*p* AOs, the orbital ionisation potentials have been taken as recommended by Charkin.[118] Eqn (35) as applied to the band structure calculations was examined first by Messmer [119] and then was successfully employed by Nishida [120] and Hoffmann et al.[121] The crucial point of this approach is a proper choice of parameters.[122] As shown below, data on the orbital exponent factors [117] and ionisation potentials [118] lead to a satisfactory description of the valence band structure of black phosphorus.

With a basis set incorporating the P *s* and *p* orbitals for four atoms in a unit cell (each atom has five valence electrons), the LCAO equation (35) yields 16 crystal orbitals; the lowest 10 of them are doubly occupied. Dispersion curves calculated for 10 occupied and two vacant crystal orbitals are shown in Fig. 28. The energy zero corresponds to the top of the valence band reached

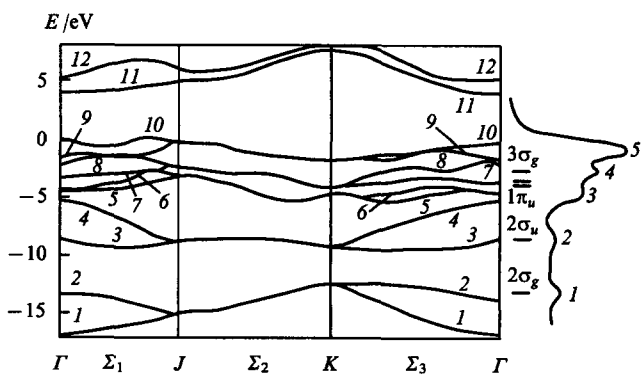


Figure 28. The dispersion curves of the energy bands in black phosphorus calculated by the extended Hückel method,[75] and from its photoelectron spectrum.[115] Horizontal lines represent levels of a cluster P_2.

near the point J along the direction Σ_1. According to the calculation, black phosphorus possesses the semiconducting properties.

The two lowest valence crystal orbitals are genetically linked with the $2\sigma_g$ IVMO of the diatomic cluster P_2, the next two, with the $2\sigma_u$ IVMO. Three pairs of the upper filled crystal orbitals originate from the $1\pi_u$ and $3\sigma_g$ OVMOs. The corresponding crystal orbitals are degenerate along the direction Σ_2. The photoelectron spectrum of a single crystal of black phosphorus obtained at a photon energy of 110 eV [115] is shown on the right side of Fig. 28.[115] Five distinct peaks sequentially spaced by 2.0, 1.9, 4.2, and 4.6 eV appear in the spectrum. All features of the photoelectron spectrum including the energies and relative heights of the peaks are represented satisfactorily by the calculated dispersion curves. The positions of MOs of the P_2 cluster at $R_{P-P}=0.2224$ nm are displayed also in Fig. 28. As is seen, the splitting of the $2\sigma_g$ and $2\sigma_u$ IVMOs composed of the P $3s$ AOs with addition of P $3p_\sigma$ AOs describes well the relative positions of peaks *2* and *1*, while the $1\pi_u$ and $3\sigma_g$ MOs fall near the centroid of peaks *3*–*5*. Thus, the qualitative features of the chemical bonding in black phosphorus crystals can be understood even in terms of diatomic interactions, i.e. in a close-order approximation, while the details of the electronic structure are determined by the band character of the wave functions.

In diatomic molecules, the orbital vibronic constants determined from spectral data can serve as a quantitative measure of the contributions of electrons to the chemical bonding. It has been shown that orbital vibronic constants correlate intimately with the orbital forces f_i [see Eqn (24)] defined as derivatives of the orbital energies $E_i(R)$ versus the interatomic distance R at the equilibrium point R_e, where i is an orbital index. Provided the orbital energies are obtained from *ab initio* calculations, the plot of orbital vibronic constant versus f_i yields a line through the coordinate origin.[53] To verify the legitimacy of this approach within the adopted semi-empirical Hoffmann method, the dependences $E_i(R)$ have been calculated [75] and the orbital forces f_i determined for N_2 (an analogue of P_2),[75] so far as the orbital vibronic constants for N_2 are available.[53, 65]

The correlation plot of the orbital vibronic constants of N_2 versus the orbital forces f_i calculated according to Eqn (24) at the experimental equilibrium distance R_e (see Refs 17, 75) is presented in Fig. 29. It may be concluded that the extended Hückel method is quite suitable for estimating the orbital vibronic constants. It has also been found that orbital vibronic constants correlate with the contributions $n(j, \mathrm{NN})$ of individual MOs to the total bond order.[53] Therefore, Mulliken orbital bond populations are also applicable to the calculation of the orbital vibronic constants. The

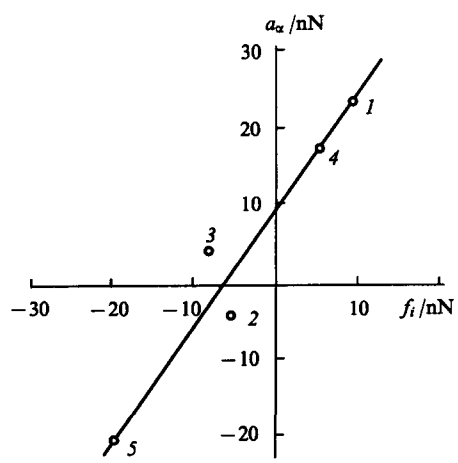


Figure 29. Dependence of the orbital vibronic constants a_α on the orbital forces f_i for N_2 (the extended Hückel calculation): (*1*) $2\sigma_g$; (*2*) $2\sigma_u$; (*3*) $2\sigma_g$; (*4*) $1\pi_u$; (*5*) $1\pi_g$.[75]

$n(j, \mathrm{NN})$–f_i correlation for N_2, a correlation which is also confirmed by calculation for P_2,[75] is evident from comparison of Fig. 29 and data from Ref. 53.

We should mention that the $2\sigma_g$ IVMO plays a particular role in the chemical bonding in P_2 as well as in N_2. Thus, orbital forces according to the EHM can be regarded as quantum-chemical indexes in the qualitative analysis of electronic contributions to chemical bonding.

As has been mentioned,[17, 75] it seems natural to extend this approach to band structure calculations for solids. To this end, a solution of the secular equation (35) is differentiated with respect to R. For the sake of convenience, two additional calculations should be carried out at $R=R_e-\Delta R$ and $R=R_e+\Delta R$, where ΔR is a small variation of the interatomic distance. The value of 0.001 nm for variations of all distances in a unit cell has been adopted in calculations of the band structure of black phosphorus. The dispersion curves obtained have been numerically differentiated with respect to R, and the orbital forces have been determined at various points of the two-dimensional Brillouin zone for the dispersion curves presented in Fig. 28. The results obtained are listed in Table 7; the average directions of Σ_1, Σ_2, and Σ_3 in the Brillouin zone are referred to these points. As follows from Table 7, the inner valence crystal orbitals *1* and *2* display slightly bonding character (the positive sign of the corresponding orbital forces). The higher crystal orbitals exhibit either a weakly-bonding (non-bonding) or antibonding (the negative sign of the orbital forces) character. The lower vacant crystal orbitals *11* and *12* possess highly antibonding character, as expected. However, the values of the orbital forces f_i depend on the coordinates of the point in the Brillouin zone. For example, at the point K, all crystal orbitals are less bonding, the inner valence crystal orbitals included. The angular dependence of the indexes of interatomic bonding f_i of crystal orbitals, e.g. *1* and *2*, can be used in studies of the anisotropy of properties of black phosphorus and other compounds.

Table 7. Orbital forces (f_i /10^{-8} N) for the energy bands of the black phosphorus.[75]

Dispersion curve number	Points of the two-dimensional Brillouin zone					
	Γ	Σ_1	J	Σ_2	K	Σ_3
12	−2.9	−3.9	−8.4	−8.3	−8.0	−7.2
11	−4.5	−6.0	−6.4	−7.3	−6.4	−4.5
10	−2.4	−2.6	−3.2	−1.7	−1.0	−2.0
9	−2.1	−1.1	−3.1	−1.7	−0.9	−1.1
8	−0.1	−1.7	−1.9	−0.6	−0.2	−1.4
7	−1.2	−1.5	−1.6	−0.6	−0.2	0.3
6	−2.1	−1.3	0.4	0.1	0.5	−0.3
5	0.7	0.6	0.4	0.1	0.5	0.6
4	0.9	0.0	0.5	−0.3	−0.1	−1.0
3	−2.1	−0.3	0.5	−0.3	−0.1	−0.9
2	2.2	1.8	1.8	1.1	−0.3	1.1
1	2.5	2.3	1.8	1.1	−0.2	1.7

The results of the study imply a prevailing contribution of the electrons of inner valence bands of atomic crystal to the covalent bonding. When considering the electronic structure of solids within the framework of the band theory, the IVMOs of the diatomic cluster, which is a building block of the crystal lattice, possess a bonding character as well.

Thus the contribution of the electrons of the inner valence MOs to the chemical bonding cannot be neglected. In certain cases, it is comparable with that of the electrons of the valence MOs.

VI. Conclusion

Widespread use of XPS in the studies of the electronic structure of molecules and solids consisting of diverse elements of the Periodic Table have provided unique results on the interaction between the electrons of the closed low-energy subshells of neighbouring atoms. In many cases, this interaction is strong enough so that one cannot neglect it in the analysis of the electronic structure of compounds. The X-ray photoelectron spectra of such compounds usually reveal a fine structure in the region of weakly-bound electrons ($\sim 15-50$ eV). The parameters of this fine structure, attributed to the inner valence electrons, reflect structural characteristics of the compounds. Experimental XPS data on the formation of IVMOs, the interrelation of the fine structure of X-ray photoelectron spectra with the structure of compounds, and the data on the participation of the inner valence electrons in chemical bonding are in good agreement with results of theoretical calculations. Qualitative interpretation of the structure of X-ray photoelectron spectra in the region of the inner valence electrons by means of group theory allows a wide range of researchers to apply XPS in various structural studies, for instance on radiation-induced damage and defects in solids.

We should note that the role of IVMOs in the formation of compounds and in the determination of their physico-chemical and structural features, has not been firmly established yet. In particular, this topic has been little covered for lanthanide and actinide series compounds. However, currently, there are several examples of the practical application of the concept of effective (experimentally observed) formation of IVMO in the explanation of experimental data. These are an inversion of the $3\sigma_g$ and $1\pi_u$ IVMOs and the exceptionally high bond strength of N_2;[51,56] the relatively broad valence band (25.2 eV) in graphite and diamond, and energies of the C–C bonds within graphite layers;[25,88] the appearance of a fine structure in the $\sim 15-50$ eV range of the X-ray photoelectron spectra of lanthanide [4,5] and actinide series [2,3,102,103] compounds; the relation of the characteristics of fine structure in X-ray photoelectron spectra of compounds containing actinide series [18,109,123] and other [17] elements with the structure of the local environment and the bond lengths to the closest ligand atoms; the appearance of a fine structure in the emission spectra of lanthanide [19] and uranium [124] compounds and in the electron conversion spectra of uranium compounds [125,126] if electrons with bonding energy within the $\sim 15-50$ eV range contribute to these spectra.

One cannot rule out [the possibility] that the formation of IVMOs in actinide series compounds explains the formation of stable groups AnO_2^{2+}. We should also note that a new method has been proposed to determine U–O distances, which can help in the identification of the products of reactions of uranium compounds with solid surfaces.[109,123,127,128]

Thus, taking into account the results considered hitherto, the following conclusions, which answer the questions listed in the 'Introduction', can be derived:

1. Under certain necessary conditions, IVMOs can form in compounds containing virtually any element of the Periodic Table.

2. The fine structure in X-ray photoelectron spectra associated with the inner valence electrons allows one to assess the contribution of electrons of the occupied AOs to the chemical bonding, the local environment of atoms under consideration, and the bond lengths in compounds.

3. In certain instances, the overall contribution of the inner valence electrons to the bond energy is comparable to that of the valence electrons. This phenomenon is novel and important for chemistry.

References

1. K Siegbahn, C Nordling, G Johansson, J Hedman, P F Heden, K Hamrin, U Gelius, T Bergmark, L O Werme, R Manne, Y Baer *ESCA Applied to Free Molecules* (Amsterdam: North-Holland, 1969)
2. Yu A Teterin, V M Kulakov, A S Baev, A G Zelenkov, I V Mel'nikov, N B Nevzorov, V A Strel'tsov, in *Tez. Dokl. Soveshchaniya "Rentgenovskie i Rentgenoelektronnye Spektry i Elektronaya Struktura Metallov, Splavov i Khimicheskikh Soedinenii"* (Abstracts of Reports of the Meeting 'X-Ray and X-Ray Electron Spectra and Electronic Structure of Metals, Alloys, and Chemical Compounds' (Izhevsk: Physicotechnical Institute, 1979) p. 25
3. Yu A Teterin, A S Baev, R V Vedrinskii, A L Gubskii, A G Zelenkov, A P Kovtun, V M Kulakov, V P Sachenko *Dokl. Akad. Nauk SSSR* **256** 381 (1981)
4. Yu A Teterin, A S Baev, V M Kulakov, A L Gubskii, A P Kovtun, S B Pirkes, G N Makushova *Dokl. Akad. Nauk SSSR* **259** 416 (1981)
5. Yu A Teterin, A S Baev, V M Kulakov, N B Nevzorov, S B Pirkes, T A Krasovskaya, in *Fizicheskie i Matematicheskie Metody v Koordinatsionnoi Khimii* (Physical and Mathematical Methods in Coordination Chemistry) (Kishinev: Shtiintsa, 1980) p. 75
6. Yu A Teterin, V M Kulakov, A S Baev, N B Nevzorov, I V Melnikov, V A Streltsov, L G Mashirov, D N Suglobov, A G Zelenkov *Phys. Chem. Miner.* **7** 151 (1981)
7. V I Nefedov, V I Vovna *Elektronnaya Struktura Khimicheskikh Soedinenii* (Electronic Structure of Chemical Compounds) (Moscow: Nauka, 1987)
8. V I Nefedov, V I Vovna *Elektronnaya Struktura Organicheskikh i Elementoorganicheskikh Soedinenii* (Electronic Structure of Organic and Organoelement Compounds) (Moscow: Nauka, 1989)
9. D V Korol'kov *Elektronnoe Stroenie i Svoistva Soedinenii Neperekhodnykh Elementov* (Electronic Structure and Properties of Compounds of Non-transition Elements) (St-Petersburg: Khimiya, 1992)
10. V M Kulakov, Yu A Teterin *Priroda (Moscow)* (2) 78 (1978)
11. L Ley, R A Pollak, S P Kowalczyk, R McFeely, D A Shirly *Phys. Rev. B, Solid State, Ser. 3* **8** 641 (1973)
12. V I Nefedov *Zh. Strukt. Khim.* **15** 1093 (1974)
13. F Jellinek, R A Pollak, M W Shafer *Matter. Res. Bull.* **9** 845 (1974)
14. B W Veal, D J Lam, W T Carnall, H R Hoekstra *Phys. Rev. B, Solid State, Ser. 3* **12** 5651 (1975)
15. E P Domashevskaya, V I Nefedov, in *Rentgenovskaya Fotoelektronnaya Spektroskopiya* (X-Ray Photoelectron Spectroscopy) (Kiev: Naukova Dumka, 1977) p. 86
16. H Heid, R Hemmel, C F Bruggen, C Haas *J. Solid State Chem.* **33** 17 (1980)
17. Yu A Teterin, S G Gagarin *Vnutrennie Valentnye Molekulyarnye Orbitali i Vliyanie ikh Elektronov na Kharakter Khimicheskoi Svyazi Soedinenii* (Inner Valence Molecular Orbitals and the Influence of Their Electrons on the Character of the Chemical Bonds in Compounds) (Moscow: TsNIIatominform, 1985)
18. Yu A Teterin, A S Baev *Rentgenovskaya Fotoelektronnaya Spektroskopiya Soedinenii Legkikh Aktinoidov* (X-Ray Photoelectron Spectroscopy of Light Actinide Compounds) (Moscow: TsNIIatominform, 1986)
19. Yu A Teterin, A S Baev *Rentgenovskaya Fotoelektronnaya Spektroskopiya Soedinenii Lantanoidov* (X-Ray Photoelectron Spectroscopy of Lantuanide Compounds) (Moscow: TsNIIatominform, 1987)
20. Yu A Teterin, in *Rentgenovskie Elektronnye Spektry i Khimicheskaya Svyaz'* (X-Ray Electron Spectra and the Chemical Bond) (Eds V V Gorchakov, V I Vovna, V I Nefedov) (Vladivostok: The Far East State University, 1986) p. 165
21. C A Coulson *Valence* (Oxford: Oxford University Press, 1961)
22. M Orchin, H H Jaffé *The Importance of Antiboding Orbitals* (Geneva: Palo Alto, 1967)
23. P Weightman, T D Thomas, D R Jennison *J. Chem. Phys.* **78** 1652 (1983)
24. W R Salaneck, R W Bigelov, H J Freund, E W Plummer *Phys. Rev. B, Condens. Matter.* **24** 2403 (1981)

25. A S Baev, A G Zelenkov, V M Kulakov, B V Odinov, V P Smilga, Yu A Teterin, Yu P Tumanov, O K Chugunov *Zh. Strukt. Khim.* **21** 29 (1980)
26. Yu A Teterin, A P Kovtun, S G Gagarin, N B Nevzorov, A S Baev, Yu P Dikov, in *Tez. dokl. 'XII Mendeleevskii S'ezd po Obshchei i Prikladnoi Khimii'* (Abstracts of Reports of the XII Mendeleev Congress on General and Applied Chemistry) (Moscow: Nauka, 1981) No 3, p. 131
27. A S Baev, V M Kulakov, Yu A Teterin, N G Gorshkov, L G Mashirov, D N Suglobov, in *Tez. dokl. 'XII Mendeleevskii S'ezd po Obshchei i Prikladnoi Khimii'* (Abstracts of Reports of the XII Mendeleev Congress on General and Applied Chemistry) (Moscow: Nauka, 1981) No 1, p. 154; *Radiokhimiya* **24** 576 (1982)
28. V A Terekhov, L N Marshakova, N P Sergushin, E M Smolyarenko, Yu A Teterin, E P Domachevskaya *Fiz. Tverd. Tela* **24** 283 (1982)
29. M Boring, J H Wood *J. Chem. Phys.* **63** 638 (1975)
30. P F Walch, D E Ellis *J. Chem. Phys.* **65** 2387 (1976)
31. V A Gubanov, A Rosen, D E Ellis *Solid State Commun.* **22** 219 (1977)
32. G L Gutsev, F F Levin *Zh. Strukt. Khim.* **20** 771(1979)
33. T Sasaki, H Adachi *Int. J. Quantum Chem.* **18** 227 (1980)
34. W Haberditzl *Basteine der Materie und Chemische Binding* (Berlin: VEB Deutscher Verlag der Wissenscaften, 1972)
35. K B Yatsimirskii, V K Yatsimirskii *Khimicheskaya Svyaz'* (The Chemical Bond) (Kiev: Vishcha Shkola, 1975)
36. L A Blyumenfel'd, A K Kukushkina *Kurs Kvantovoi Khimii i Stroenie Molekul* (Textbook of Quantum Chemistry and Molecular Structure) (Moscow: Izd. Moskovsk. Gos. Univ., 1980)
37. Yu N Kukushkin, E I Maslov *Stroenie Atomov i Khimicheskaya Svyaz'* (The Structure of Atoms and the Chemical Bond) (Leningrad: Izd. Leningradsk. Gos. Univ., 1973)
38. J N Murrell, S F A Kettle, J M Tedder *Valence Theory* (New York: Wiley, 1965)
39. M J S Dewar, R C Dougherty *The PMO Theory of Organic Chemistry* (New York: Plenum, 1975)
40. V I Minkin, B Ya Simkin, R M Minyaev *Teoriya Stroeniya Molekul (Elektronnye Obolochki)* [The Molecular Structure Theory (Electron Shells)] (Moscow: Vysshaya Shkola, 1979)
41. K S Krasnov *Molekuly i Khimicheskaya Svyaz'* (Molecules and the Chemical Bond) (Moscow: Vysshaya Shkola, 1977)
42. G Henrici-Olivé, S Olivé *Coordination and Catalysis* (Wainheim: Verlag Chemie, 1977)
43. F A Cotton, G Wilkinson *Advanced Inorganic Chemistry* (New York: Interscience, 1966)
44. E Cartmell, G W A Fowles *Valence and Molecular Structure* (London: Butterworth, 1978)
45. T I Krasovitskaya *Elektronnye Struktury Atomov i Khimicheskaya Svyaz'* (The Electronic Structures of Atoms and the Chemical Bond) (Moscow: Prosveshchenie, 1980)
46. V I Kornev, M N Konyukhov *Stroenie Atoma i Priroda Khimicheskoi Svyazi* (The Structure of the Atom and the Nature of the Chemical Bond) (Izhevsk: Physicotechnical Institute, 1972)
47. M Kotani, K Ohno, K Kayama, in *Handbuch der Physik* Vol. 37/2 (Berlin: Springer, 1961) p. 173
48. R D Harcourt *Qualitative Valence-Bond Descriptions of Electron-Rich Molecules: Pauling '3-Electron Bonds' and 'Increased-Valence' Theory* (Berlin: Springer, 1982)
49. M S Gopinathan, C Ravimohan *Chem. Phys. Lett.* **85** 307 (1982)
50. K Hermann, P S Bagus, C R Brundle, D Menzel *Phys. Rev. B, Condens. Matter* **24** 7025 (1981)
51. Yu A Teterin, S G Gagarin, Yu P Dikov, G L Gutsev *Dokl. Akad. Nauk SSSR* **268** 921 (1983)
52. Yu A Teterin, A S Baev, S G Gagarin, A P Kovtun *Dokl. Akad. Nauk SSSR* **273** 156 (1983)
53. S G Gagarin, Yu A Teterin, Yu P Dikov *Zh. Fiz. Khim.* **57** 2624 (1983)
54. V A Gubanov, A Rosen, D E Ellis *J. Inorg. Nucl. Chem.* **41** 975 (1979)
55. G M Zhidomirov, A A Bagatur'yants, I A Abronin *Prikladnaiya Kvantovaya Khimiya* (Applied Quantum Chemistry) (Moscow: Khimiya, 1979)
56. Yu A Teterin, S G Gagarin, Yu P Dikov, G L Gutsev, V V Nemoshkalenko *Teor. Eksp. Khim.* **19** 259 (1983)
57. S G Gagarin, I A Lygina, in *Kvantovaya Khimiya* (Quantum Chemistry) (Kishenev: Shtiintsa, 1975) p. 50
58. R F W Bader, W H Henneker, P E Cade *J. Chem. Phys.* **46** 3341 (1967)
59. A M Gul'maliev, I V Stankevich *Zh. Fiz. Khim.* **46** 2711 (1972)
60. K Ruedenberg *J. Chem. Phys.* **66** 375 (1977)
61. O Goscinski, in *Quantum Science. Methods and Structure* (Eds J-L Calais, O Goscinski, J Linderberg, Y Ohrn) (New York: Plenum, 1976) p. 427
62. S G Gagarin *Koord. Khim.* **6** 215 (1980)
63. I B Bersuker *Kinet. Katal.* **18** 1268 (1977)
64. S G Gagarin, Yu A Teterin *Zh. Strukt. Khim.* **25** (4) 125 (1984)
65. S G Gagarin, Yu A Teterin *Zh. Strukt. Khim.* **25** (6) 18 (1984)
66. P E Cade, K D Sales, A C Wahl *J. Chem. Phys.* **44** 1973 (1966)
67. R K Nesbet *J. Chem. Phys.* **40** 3619 (1964)
68. H Lefebvre-Brion, C M Moser, R K Nesbet *Chem. Phys.* **34** 1950 (1961)
69. P E Cade, W M Huo *J. Chem. Phys.* **47** 614 (1967)
70. S G Gagarin, Yu A Teterin *Zh. Fiz. Khim.* **58** 3015 (1984)
71. S G Gagarin, Yu A Teterin *Zh. Neorg. Khim.* **29** 1915 (1984)
72. Yu A Teterin, A D Sidorenko, S G Gagarin, in *Kvantovaya Khimiya Tverdogo Tela. Preprint UNTs AN SSSR* (Quantum Chemistry of Solids. Preprint of the Ural Scientific Centre of the Academy of Sciences of the USSR) (Sverdlovsk, 1984) p. 55
73. S G Gagarin, Yu A Teterin, in *Kvantovaya Khimiya Tverdogo Tela. Preprint UNTs AN SSSR* (Quantum Chemistry of Solids. Preprint of the Ural Scientific Centre of the Academy of Sciences of the USSR) (Sverdlovsk, 1984) p. 58; *Teor. Eksp. Khim.* **21** 211 (1985)
74. S G Gagarin, Yu A Teterin *Zh. Fiz. Khim.* **59** 920 (1985)
75. S G Gagarin, Yu A Teterin, in *Kvantovaya Khimiya Tverdogo Tela. Preprint UNTs AN SSSR* (Quantum Chemistry of Solids. Preprint of the Ural Scientific Centre of the Academy of Sciences of the USSR) (Sverdlovsk, 1984) p. 68; *Zh. Strukt. Khim.* **26** (4) 54 (1985)
76. Yu A Teterin, M V Ryzhkov, V A Gubanov, S G Gagarin, in *Kvantovaya Khimiya Tverdogo Tela. Preprint UNTs AN SSSR* (Quantum Chemistry of Solids. Preprint of the Ural Scientific Centre of the Academy of Sciences of the USSR) (Sverdlovsk, 1984) p. 62
77. Yu A Teterin, M V Ryzhkov, V A Gubanov, S G Gagarin, in *Voprosy Atomnoi Nauki i Tekhniki (Ser. Obshchaya i Yadernaya Fizika)* [Problems in Atomic Science and Engineering (General and Nuclear Physics Ser.)] (Moscow: TsNIIatominform, 1984) Vol. 4, No 29, p. 91; *Dokl. Akad Nauk SSSR* **284** 915 (1985)
78. Yu A Teterin, Doctoral Thesis in Physicomathematical Sciences, Institute of Chemical Physics of the Academy of Sciences of the USSR, Moscow, 1989
79. M V Ryzkov, V A Gubanov, Yu A Teterin, A S Baev *Phys. Rev. B, Condens. Matter.* **59** 1; 7 (1985)
80. M V Ryzhkov, V A Gubanov, Yu A Teterin, A S Baev *Zh. Neorg. Khim.* **30** 2475 (1985)
81. Yu A Teterin, A S Baev, S G Gagarin, V D Klimov *Radiokhimiya* **27** 3 (1985)
82. Yu A Teterin, A S Baev, S G Gagarin *Radiokhimiya* **28** 318 (1986)
83. Yu A Teterin, A S Baev, L G Mashirov, D N Suglobov *Radiokhimiya* **28** 460 (1986)
84. Yu A Teterin, A S Baev, L G Mashirov, D N Suglobov, in *Voprosy Atomnoi Nauki i Tekhniki (Ser. Obshchaya i Yadernaya Fizika)* [Problems in Atomic Science and Engineering (General and Nuclear Physics Ser.)] (Moscow: TsNIIatominform, 1986) Vol. 36, No 3, p. 60
85. A S Baev, Yu A Teterin, in *Voprosy Atomnoi Nauki i Tekhniki (Ser. Obshchaya i Yadernaya Fizika)* [Problems in Atomic Science and Engineering (General and Nuclear Physics Ser.)] (Moscow: TsNIIatominform, 1986) Vol. 36, No 3, p. 60
86. J Schirmer, L S Cederbaum, W Domcke, W Von Niessen *Chem. Phys.* **26** 149 (1977)
87. N Honjou, T Sasajima, F Sasaki *Chem.Phys.* **57** 475 (1981)
88. Yu A Teterin, S G Gagarin, A S Baev, in *Poverkhnostnye i Teplofizicheskie Svoistva Almazov. Preprint ISM AN USSR* (Surface and Thermal Properties of Diamonds. Preprint of the Institute of Structural Materials of the Academy of Sciences of Ukr. SSR) (Kiev, 1985) p. 17
89. M I Sosulnikov, Yu A Teterin *J. Electron. Spectrosc. Relat. Phenom.* **59** 111 (1992)
90. Yu A Teterin, M I Sosulnikov *Appl. Supercond.* **3–6** 457 (1993)

91. Yu A Teterin, M I Sosulnikov, Yu A Petrov *J. Electron. Spectrosc. Relat. Phenom.* **68** 469 (1994)
92. Yu A Teterin, M I Sosulnikov, L D Shustov *J. Electr. Spectr. Relat. Phenom.* **68** 453 (1994)
93. Yu A Teterin, V M Kulakov, V V Lomonosov, A S Baev, M I Sosul'niiov, in *Voprosy Atomnoi Nauki i Tekhniki. (Ser. Yaderno-Fizicheskie Issledovaniya)* [Problems in Atomic Science and Engineering (Nuclear-Physical Investigations Ser.)] (Moscow: TsNIIatominform, 1990) Vol. 5, No 13, p. 71
94. Yu A Teterin, A S Baev, M I Sosul'nikov, Yu N Simirskii *Sverkhprovodimost: Fiz., Khim., Tekhnika* (3) 25 (1988)
95. V M Ryzhkov, N I Medvedeva, A F Golota, M Ya Khodos, V A Gubanov *Zh. Strukt. Khim.* **26** (6) 76 (1985)
96. Yu A Teterin, V M Kulakov, A S Baev, A G Zelenkov, N B Nevzorov, I V Mel'nikov, V A Strel'tsov, L G Mashirov, D N Suglobov *Dokl. Akad. Nauk SSSR* **255** 434 (1980)
97. B C Frazer, G Shirane, D E Cox, C E Olsen *Phys. Rev. A* **140** 1448 (1965)
98. J C Fuggle, A F Burr, L M Watson, D J Fabian, W Lang *J. Phys. F* **4** 335 (1974)
99. K N Huang, M Aojagi, M N Chen, B Crasemann, H Mark *At. Data Nucl. Data Tabl.* **18** 243 (1976)
100. J J Pireaux, N Martensson, R Didriksson, K Siegbahn, J Riga, J Verbist *Chem. Phys. Lett.* **46** 215 (1977)
101. Yu A Teterin, A S Baev, in *Voprosy Atomnoi Nauki i Tekhniki (Ser. Obshchaya i Yadernaya Fizika)* [Problems in Atomic Science and Engineering (General and Nuclear Physics Ser.)] (Moscow: TsNIIatominform, 1985) Vol. 4, No 33, p. 53
102. Yu A Teterin, A S Baev, L G Mashirov, D N Suglobov *Dokl. Akad. Nauk SSSR* **276** 154 (1984)
103. Yu A Teterin, A S Baev, L G Mashirov, D N Suglobov *Dokl. Akad. Nauk SSSR* **277** 131 (1984)
104. Yu A Teterin, A S Baev, A D Sidorenko, S G Gagarin, in *Rentgenovskaya Spektroskopiya Tverdogo Tela. Preprint UNTs AN SSSR* (X-Ray Spectroscopy of Solids. Preprint of the Ural Scientific Centre of the Academy of Sciences of the USSR) (Sverdlovsk, 1984) p. 23
105. J H Scofield *J. Electron. Spectrosc. Relat. Phenom.* **8** 129 (1976)
106. A L Gubskii, A P Kovtun, Yu A Teterin, A S Baev *Elektronnoe Stroenie i Struktura RES Uranilovykh Soedinenii. Preprint IAE* (Electronic Structure of X-Ray Electron Spectra of Uranyl Compounds. Preprint of the Institute of Atomic Energy) (Moscow, 1984) No 4053/12
107. V A Glebov *Elektronnoe Stroenie i Svoistva Uranilovykh Soedinenii* (Electronic Structure and Properties of Uranyl Compounds) (Moscow: Energoatomizdat, 1983)
108. G V Ionova, V G Pershina, V I Spitsin *Elektronnoe Stroenie Aktinoidov* (Electronic Structure of the Actinides) (Moscow: Nauka, 1986)
109. Yu A Teterin, A S Baev, S A Bogatov *J. Electron. Spectrosc. Relat. Phenom.* **68** 685 (1994)
110. Yu A Teterin, A S Baev, N G Yakovlev, in *Voprosy Atomnoi Nauki i Tekhniki (Ser. Obshchaya i Yadernaya Fizika)* [Problems in Atomic Science and Engineering (General and Nuclear Physics Ser.)] (Moscow: TsNIIatominform, 1992) Vol. 3, p. 58
111. M V Ryzhkov, V A Gubanov, Yu A Teterin, A S Baev *Radiokhimiya* **33** (1) 22 (1991); **34** (1) 85 (1992)
112. Yu A Teterin, S G Gagarin, in *Voprosy Atomnoi Nauki i Tekhniki (Ser. Obshchaya i Yadernaya Fizika)* [Problems in Atomic Science and Engineering (General and Nuclear Physics Ser.)] (Moscow: TsNIIatominform, 1984) Vol. 4, No 29, p. 89
113. P E Cade, A C Wahl *At. Data Nucl. Data Tables* **13** 339 (1974)
114. A Brown, S Rundqvist *Acta Crystalogr.* **19** 684 (1965)
115. M Taniguchi, S Suga, M Seki, H Sakamoto, H Kanzaki, Y Alkahama, S Terada, S Endo, S Narita *Solid State Commun.* **45** 59 (1983)
116. S G Gagarin *Zh. Fiz. Khim.* **57** 1212 (1983)
117. E Clementi, D L Raimondi *J. Chem. Phys.* **38** 2686 (1963)
118. O P Charkin *Stabil'nost' i Struktura Gazoobraznykh Neorganicheskikh Molekul, Radikalov i Ionov* (Stability and Structure of Inorganic Gaseous Molecules, Radicals, and Ions) (Moscow: Nauka, 1980)
119. R P Messmer *Chem. Phys. Lett.* **11** 589 (1971)
120. M Nishida *Phys. Rev. B, Solid State, Ser. 3* **95** 263 (1979)
121. L A Grunes, R D Leapman, C N Hoffmann, A B Kunz *Phys. Rev. B, Condens. Matter* **5** 7157 (1982)
122. S G Gagarin, Yu A Kolbanovskii *Kinet. Katal.* **23** 1454 (1982)
123. Yu A Teterin, A S Baev, K E Ivanov, L G Mashirov, D N Suglobov *Radiokhimiya* **38** (4) 365 (1996)
124. Yu A Teterin, V A Terekhov, K E Ivanov *Dokl. Akad. Nauk* **345** 365 (1995)
125. V I Zhudov, A G Zelenkov, V M Kulakov, B V Odinov, Yu A Teterin, in *Tez. Dokl. XXX Vsesoyuz. Soveshchaniya po Yadernoi Spektroskopii i Strukture Atomnogo Yadra* (Abstracts of Reports of the XXX All-Union Conference on Nuclear Spectroscopy and the Structure of the Atomic Nucleus) (Leningrad: Nauka, 1980) p. 614
126. D P Grechukhin, V I Zhudov, A G Zelenkov, V M Kulakov, B V Odinov, A A Soldatov, Yu A Teterin *Pis'ma Zh. Eksp. Teor. Fiz.* **31** 627 (1980)
127. Yu A Teterin, V I Nefedov, K E Ivanov, A S Baev, G Gaipel', T Raikh, Ch Niche *Dokl. Akad. Nauk* **344** 206 (1995)
128. V I Nefedov, Yu A Teterin, T Raikh, Kh Niche *Dokl. Akad. Nauk* **348** 634 (1996)